NASA CONTRACTOR REPORT

NASA CR-2565

DEVELOPMENT OF A SUPERCONDUCTOR MAGNETIC SUSPENSION AND BALANCE PROTOTYPE FACILITY FOR STUDYING THE FEASIBILITY OF APPLYING THIS TECHNIQUE TO LARGE SCALE AERODYNAMIC TESTING, FINAL REPORT

R. N. Zapata, R. R. Humphris, and K. C. Henderson

Prepared by
UNIVERSITY OF VIRGINIA, UNIV., RES. LABS. FOR THE ENGINEERING SCIENCES
Charlottesville, Va. 22901
for Langley Research Center

NATIONAL AERONAUTICS AND SPACE ADMINISTRATION • WASHINGTON, D. C. • JULY 1975

1. Report No.	2. Government Accession No.	3. Recipient's Catalog No.
NASA CR-2565		

4. Title and Subtitle	5. Report Date
Development of a Superconductor Magnetic Suspension and Balance Prototype Facility for Studying the Feasibility of Applying this Technique to Large-Scale Aerodynamic Testing	July 1975
	6. Performing Organization Code
7. Author(s)	8. Performing Organization Report No.
R. N. Zapata, R. R. Humphris, and K. C. Henderson	
9. Performing Organization Name and Address	10. Work Unit No.
Department of Engineering Science and Systems Research Laboratories for the Engineering Sciences School of Engineering and Applied Science University of Virginia, Charlottesville, Va. 22901	505-06-42-02
	11. Contract or Grant No.
	NGR 47-005-112
12. Sponsoring Agency Name and Address	13. Type of Report and Period Covered
National Aeronautics and Space Administration Washington, D. C. 20546	Contractor Report Sept. 1, 1969-Sept. 30, 1974
	14. Sponsoring Agency Code

15. Supplementary Notes

Final report.

16. Abstract

Magnetic suspension techniques have proved very useful for simulating free-flight conditions in wind tunnels for nearly 20 years. However, application of such techniques to high Reynolds number aerodynamic testing has been impeded so far by unmanageable design requirements on conventional support magnets imposed by the large sizes and high aerodynamic loads which are characteristic of experiments in the high Re regime. In this report, unique design and operational characteristics of a prototype magnetic suspension and balance facility which utilizes superconductor technology are described and discussed from the point of view of scalability to large sizes. The successful experimental demonstration of the feasibility of this new magnetic suspension concept of the University of Virginia, together with the success of the cryogenic wind-tunnel concept developed at Langley Research Center, appear to have finally opened the way to clean-tunnel, high-Re aerodynamic testing. Results of calculations corresponding to a two-step design extrapolation from the observed performance of the prototype magnetic suspension system to a system compatible with the projected cryogenic transonic research tunnel are presented to give an order-of-magnitude estimate of expected performance characteristics. Research areas where progress should lead to improved design and performance of large facilities are discussed.

17. Key Words (Suggested by Author(s)) (STAR category underlined)	18. Distribution Statement
Magnetic suspension Superconductivity Wind tunnel	Unclassified - Unlimited Subject Category 02 Aerodynamics

19. Security Classif. (of this report)	20. Security Classif. (of this page)	21. No. of Pages	22. Price*
Unclassified	Unclassified	64	$4.25

*Available from { The National Technical Information Service, Springfield, Virginia 22151
STIF/NASA Scientific and Technical Information Facility, P.O. Box 33, College Park, MD 20740

TABLE OF CONTENTS

TABLE OF CONTENTS - CONTINUED

FOREWORD

This long standing project has had a good share of happy and exciting moments, when different stages of success in the laboratory crowned long sustained effort which included creativity, persistance, and plain hard work. But, unfortunately, there have been more than a normal share of sad moments. Three people associated with the project have passed away. Bob Russell, who took initial responsibility for the design and implementation of power supplies to drive the coil system, died tragically in September of 1968. Then, in December of 1973, Harleth Wiley, the long time promoter of wind tunnel magnetic suspension research and to whom this entire project is enormously indebted in so many ways, passed away. Finally, in September of 1974, Hermon Parker died. Hermon was the creative intellectual force behind the University of Virginia magnetic suspension concept, which he first discovered in 1959. He was the author of practical scaling laws for magnetic coils and was the first to champion the "cold balance" concept. He also saw the potential of iron cores in aerodynamic models and did extensive research on the feasibility of utilizing iron vis-a-vis the requirements of the quasi six-degree-of-freedom testing concept for dynamic stability studies. This author was fortunate to be associated professionally with Hermon Parker and to enjoy his personal friendship as well. Words are inadequate to describe the loss his untimely death means to all of us present and past members of this research team. Rather, in the knowledge that this project meant so much to him and the realization of his pioneering concepts gave him so much personal satisfaction, this final technical report is dedicated to his memory.

R. N. Zapata
January 1975

I. INTRODUCTION

This report is concerned with basic research and development work towards proving the feasibility of operating an all-superconductor magnetic suspension and balance device for aerodynamic testing. There were originally two principal objectives guiding this work, i.e., (1) to study the feasibility of applying a quasi-six-degree-of-freedom free support technique to dynamic stability research, and (2) to investigate design concepts and parameters that appear critical for applying magnetic suspension techniques to large-scale aerodynamic facilities. As time progressed it became practical to shift the relative emphasis between these two objectives more and more in favor of the second one. Hence, although the validity of this approach and the legitimacy of our group interest concerning dynamic stability research have never been seriously questioned it will be obvious from the tone and the bulk of the content of this report that our most vigorous efforts have been devoted to the pursuit of the second objective. To put this final report into proper perspective it is appropriate to keep in mind that work supported by this NASA Grant NGR 47-005-112 is a continuation of work supported by NASA Grant NGR 47-005-029 and is currently being followed up under NASA Grant NGS-1010. Overall, the development of this unique prototype aerodynamic test facility took about eight years from the initial formal design studies to complete implementation, although it is hard to pin down an exact length of time because the current follow up of work started under the grant for which this final report is written, is intimately connected with further development and refinement of the basic prototype facility.

However, the official termination date for Grant 47-005-112 (September 30, 1974) does mark a definite change of emphasis from research effort centered on the prototype facility proper to research effort on scaling of compoments for a larger facility. Furthermore, the definitive proof-of-concept experiments took place in the middle of the grant period which extended from September 1, 1969 to September 30, 1974.

During the five years covered in this report, our research group published several papers and reported periodically to NASA on current progress. Thus, most of the significant results delivered have already been communicated either in the open literature or in direct communications to NASA. There is merit though, in bringing together in one report, however briefly, all relevant aspects of the development of the prototype facility, such that a self-contained comprehensive description results. This is the goal of the present report. Its main body is divided into three sections, i.e., Design Characteristics, Operational Characteristics, and Scaling to Larger Facilities. A list of relevant publications by members of the University of Virginia research group is included at the end of the report.

2. DESIGN CHARACTERISTICS

A. A magnetic suspension and balance system is a rather complex device even if conventional technology is utilized. In the present case, state-of-the-art technology was explored and adopted for several key components of the final system. This tended to parcel out our design efforts in rather well defined separate packages which, of course, had to be integrated into the overall system. The description below is given in terms of these different component parts and borrows heavily from reference (4).

2.1 Coil System

The design of our prototype facility evolved from the concept of a cold magnetic suspension and balance first proposed by Parker in 1966 (1). The basic idea was to reduce size and power dissipation (and hence construction and operational cost) of supporting and magnetizing coils by reducing the resistivity of conductors used to wind such coils. Dramatic reductions were predicted for a coil system utilizing high purity copper operated at 20°K. Parker illustrated this concept with a highly symmetric coil configuration with excellent characteristics for use as a force balance as well as a model suspension. The basic operating principle of this magnetic suspension and balance is easily explained

with the aid of Figures 1 and 2. A perfect sphere of isotropic ferromagnetic material, when placed in a uniform magnetic field becomes uniformly magnetized. Since the magnetizing field is uniform it exerts no force on the magnetized sphere. A force does result if a magnetic field with a gradient is added. This can be produced efficiently by a pair of coils, wound on a common symmetry axis, placed symmetrically about the sphere, and with equal but opposite currents. Such an arrangement produces no field but maximum field gradient at the sphere center, proportional to the current for air-core coils.

The direction and the magnitude of the force on the sphere depend on the angle ϕ between the gradient coil pair axis and the direction of magnetization of the sphere. The fundamental relationship is:

$$d\vec{F} = (d\vec{M} \cdot \nabla)\, \vec{B}$$

where $d\vec{F}$ is the element of force acting on an element $d\vec{M} = \vec{M}\, dV$ of magnetized material of volume dV in an external field $\vec{B}$. Assuming that the gradient field is axially symmetrical about the gradient coil axis which passes through the center of the sphere, no moment of force acts on the sphere and the force on the sphere is in the plane defined by the direction of $\vec{M}$ (or $\vec{B}$, in this case) and the gradient coil axis.

In Figure 2 the two special cases of coil configurations which yield three orthogonal force directions are noted. The first configuration consists of two pairs of $\phi = \tan^{-1}\sqrt{2}$ coils and one pair of $\phi = 0$ coils. This coil arrangement (somewhat modified) has been used successfully by Zapata and Dukes at Princeton (2). The second configuration consists of three pairs of gradient coils placed symmetrically about the sphere magnetization axis at an angle $\phi = \tan^{-1}\sqrt{8}$. The three orthogonal force directions lie along the edges of a cube whose major diagonal coincides with the magnetization axis. This configuration provides the maximum space for placing a wind tunnel inside the coil assembly, with the flow direction aligned with the sphere magnetization vector. This is the configuration adopted for the prototype facility developed at the University of Virginia.

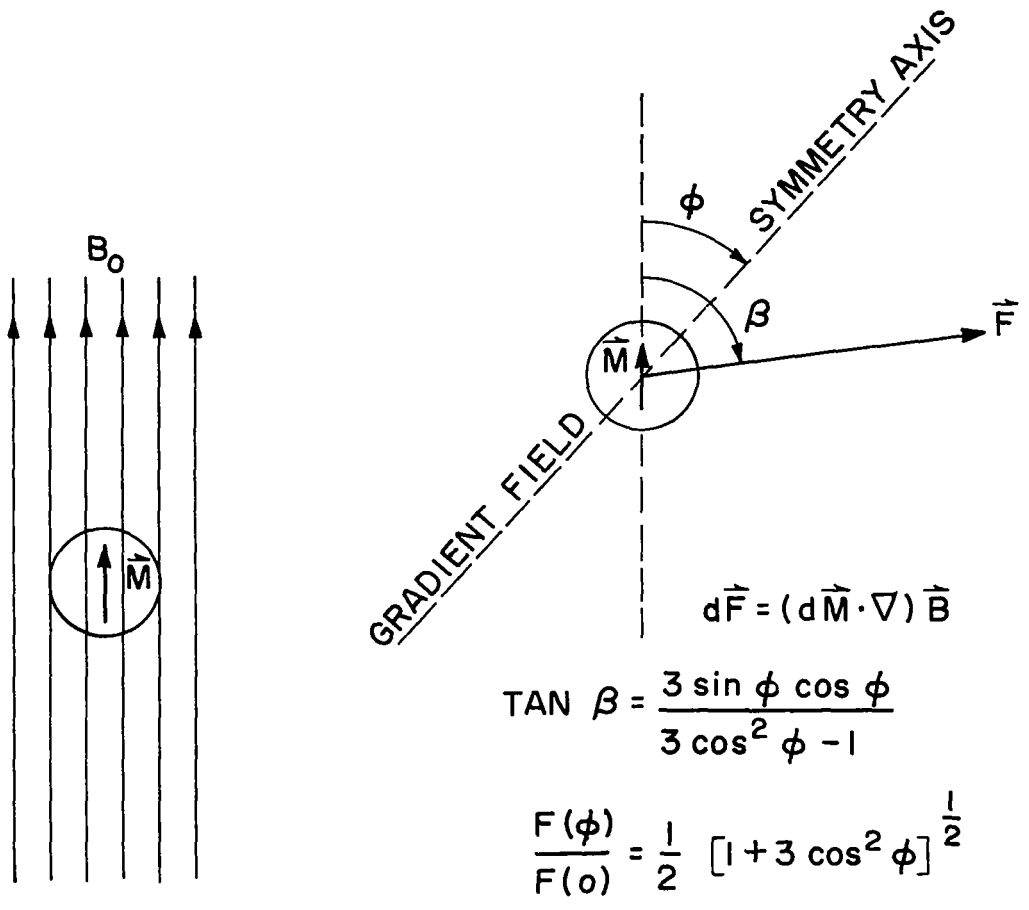

Figure 1 University of Virginia Magnetic Suspension Principle.

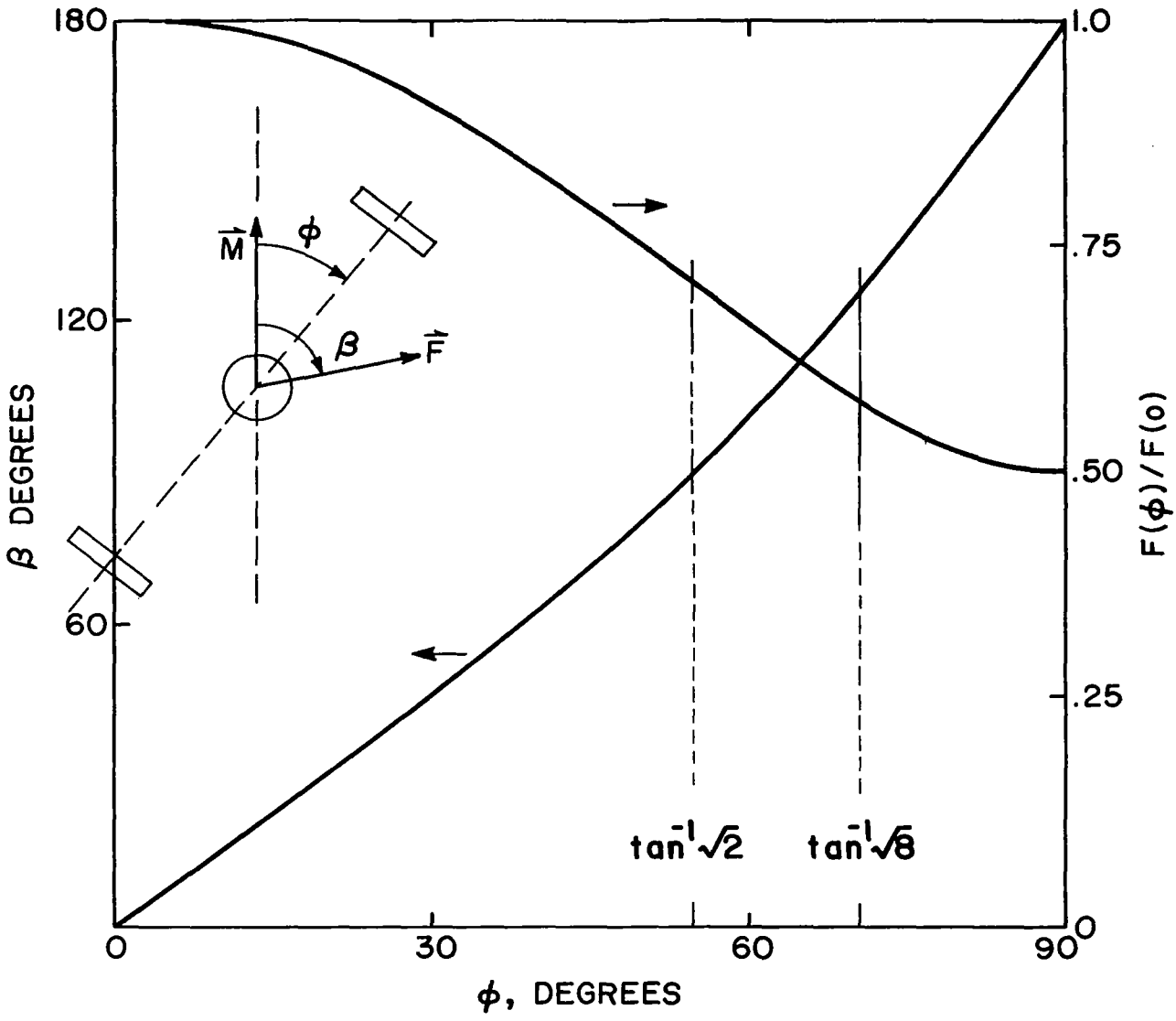

Figure 2 Force Direction and Magnitude versus ϕ.

The transition from simply cold (or, more precisely, supercooled) normal conductors to superconductors operating at liquid helium temperature was motivated by the desire to test in the prototype facility as much of the technology estimated to be needed for large scale facilities as possible. A discussion of some of the problems associated with using supercooled high purity conductors may be found in reference (3). A comprehensive, updated discussion on the relative merits of supercooled vs. superconductor suspension systems for intermediate size facilities is currently being prepared under Grant NSG-1010 and will be published as a separate progress report in early 1975.

The greatest uncertainty concerning the utilization of superconductors for wind tunnel magnetic suspension and balance systems was the level of energy dissipation (and hence, helium boil-off) associated with a.c. operation in the tightly coupled dynamic environment typical of such systems. At the same time, this a.c. behavior constituted the most critical design parameter vis-a-vis feasibility of this entire magnetic suspension concept, including safety and economic considerations. Hence, it follows that the most significant contribution we claim in this report is the removal of this uncertainty and the experimental proof of the feasibility of using superconductors in this type of dynamic operation.

A dimensional sketch of the coil assembly of the prototype facility is given in Figure 3. Cross sections of the main field coil, both drag augmentation coils, and one gradient coil pair are shown together with contours of the wind tunnel and the liquid nitrogen and liquid helium dewars. Principal dimensions and other design characteristics of the coils are summarized in Table I.

2.2 Cryogenic System

The requirement of providing a liquid helium environment for the operation of the superconducting coils is satisfied by a cryogenic subsystem consisting of three principal components: a helium cryostat, a set of vapor-cooled current leads, and appropriate pressure and temperature instrumentation. This cryogenic subsystem is the least

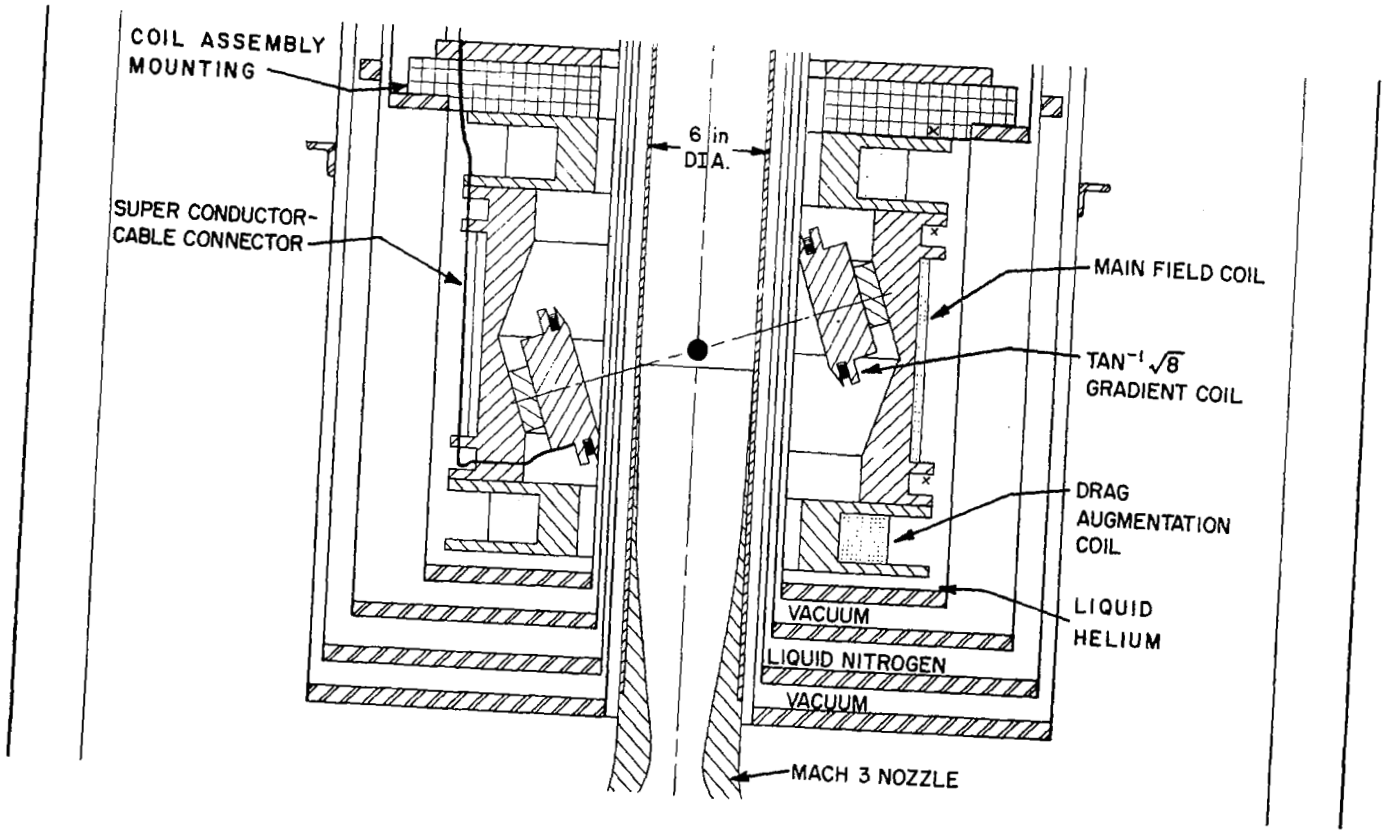

Figure 3 Sketch of Superconductor Coil Configuration

TABLE I

Prototype Coil Characteristics

PROPERTIES	COIL TYPES: GRADIENT	DRAG AUGMENTATION	MAIN FIELD
Number of coils in assembly	6	2	1
Number of turns/coil	135	3200	2500
Dimensions, OD/ID/L (cm)	20/13/1.3	51/38/6.4	57/55/25
Type of superconductor	GE-150 NbSn tape	0.076 cm copper clad NbTi single strand wire	
Type of operation	a.c.	d.c.	d.c.
Measured resistance room temp./ L He temp. (Ω)	1.9/0.0012 (1 coil)	423/0.0033 (2 coils)	203/0.0036
Measured inductance room temp./ L He temp. (Ω)	$3.9\times10^{-3}/3.6\times10^{-3}$ (1 coil)	7.6/4.4 (2 coils)	2.2/1.6
Measured Q-factor room temp./ L He temp. (Ω)	8/25	2.1/4.2	2.2/2.6
Maximum design current (A)	350	100	100
Maximum mag. field at NSP (G) (1 coil)	575	3200	6100
Maximum mag. field gradient at NSP (G/cm) (1 coil)	36	210	0

(NSP: Nominal Suspension Point)

conventional component of the prototype facility and has, at the same time, influenced the design of several other components quite markedly. For this reason, it is appropriate that the following discussion be sufficiently comprehensive even at the risk of making it somewhat lengthy.

Experimental helium cryostats must meet the basic specification for a storage dewar, i.e., hold a prescribed quantity of liquid helium with minimum refrigeration losses that occur chiefly by conduction and radiation mechanisms. Conduction losses are minimized by (a) constructing the cryogenic vessel with thin, low thermal-conductivity materials, (b) surrounding the liquid container with a hard-vacuum jacket, and (c) careful design of leads and internal supports connecting low and high temperature regions. Radiation losses are minimized by either of two methods: (1) surrounding the liquid container with a wall held at an intermediate temperature (typically, liquid nitrogen temperature), (2) interposing a series of reflecting surfaces or shields between the liquid container wall and the (room temperature) outside wall; often a combination of both these methods is used for increased effectiveness.

Aside from the foregoing specification, the prototype cryogenic unit must satisfy the following functional constraints: (i) room temperature access for the supersonic wind tunnel, the model position sensor, and other system components must be provided, (ii) the distance between the coils and the wind tunnel should be kept as short as possible, (iii) interference with the magnetic interaction between the coils and the suspended model must be avoided, (iv) accessibility to the coils and other components inside the dewar must be reasonably good. Finally, a common specification for experimental systems, high reliability, assumes special importance in this case.

Without going into excessive detail, consider a few of the most significant consequences of these specifications. For example, constraint (i) leads to a generalized annular geometry in potential conflict with constraints (ii) and (iii), since the inside walls of the annulus will stand between the coils and the suspended model. Furthermore, the possibility of using a simple radiation barrier around the helium

container (typically, a copper skirt held at liquid nitrogen temperature, located inside a single vacuum jacket), is eliminated since the eddy currents induced in such a high thermal-and electrical-conductivity barrier will surely interfere with the interaction between the coils and the model. An alternate solution consisting of packing superinsulation (aluminized mylar) in the vacuum jacket surrounding the helium vessel has to be eliminated for the same reason. The only remaining practical solution uses a liquid-nitrogen radiation shield; however, this solution increases considerably the complexity of the design of the cryostat, since it requires four walls between the liquid helium environment and the room temperature environment. This solution is still in potential conflict with constraints (ii) and (iii) as can be appreciated upon examination of Figure 3. The cylindrical inner walls of this cryostat (shown as vertical lines in the figure) are very thin and are spaced very closely to one another in an effort to meet constraint (ii). Originally, all four inner tubes were made of fiberglass-epoxy bonded to the rest of the cryogenic vessel by a special process. It must be remembered at this point that the effectiveness of a liquid helium dewar depends most critically on the tightness of the vacuum jacket surrounding the liquid container. Even small leaks (by more conventional standards) cannot be tolerated. At the same time, the success of this entire electromagnetic balance concept hinges upon the ability to operate the balance without excessive helium losses. Consequently, when a vacuum leak developed in one of the fiberglass tubes of the inner vacuum jacket, and resisted all attempts to repair it, both tubes of that vacuum jacket were replaced by non-magnetic stainless steel tubes. Experiments conducted to determine the nature and magnitude of the effect of the presence of these (metal) walls on the magnetic interaction between the coils and the model, revealed that magnetic field attenuation and phase shift associated with eddy currents induced in these walls, were of small but finite magnitude. As expected, these effects are accentuated as the frequency of the coil current increases. These experiments are documented in reference 3.

The dewar is physically separable into two parts: the inner, or liquid helium dewar, and the outer, or liquid nitrogen dewar. This characteristic proved invaluable at the time the leak in the inner dewar was detected and subsequently fixed. Unless there is a reason to separate them, normally both parts stay together when the coil assembly is removed from the system. When the system is fully assembled, both these parts are independently fastened to the top plate that supports the entire assembly (see Figure 4).

A set of 10 current leads carries electric current from the outside of the dewar to the nine coils inside. These leads are specially designed to use the cooling power of helium vapor to maximum advantage by serving as outlets for the helium boil-off. One such vapor-cooled lead is shown in Figure 4. In principle, for every current distribution in the coil system there is an optimum distribution of helium vapor flow rate through the vapor-cooled leads that minimizes the total helium boil-off in the dewar. In practice, if the leads are adequately sized, it is not necessary to monitor the vapor flow distribution, but it is only necessary to monitor the temperature of the outflowing vapor to detect gross unbalances indicative of severe malfunctions. In this facility all vapor-cooled leads are equipped with thermocouples at the ends leading out of the dewar; in addition, all connecting tubes between the leads and the helium recovery manifold are individually valved to facilitate any necessary adjustments. The details of the design of the vapor-cooled leads can be found in a publication by Efferson (5) from which all the information needed to fabricate the leads for this facility was obtained.

The instrumentation requirements for the cryogenic subsystem are better understood by considering some of its key operational aspects. For example, since liquid helium is considerably more expensive than liquid nitrogen, it is common practice, specially when large systems are involved, to pre-cool the system to liquid nitrogen temperature before starting the transfer of liquid helium into the system. This pre-cooling process can be accelerated by bleeding dry nitrogen into the vacuum jacket between the liquid helium and liquid nitrogen containers until the

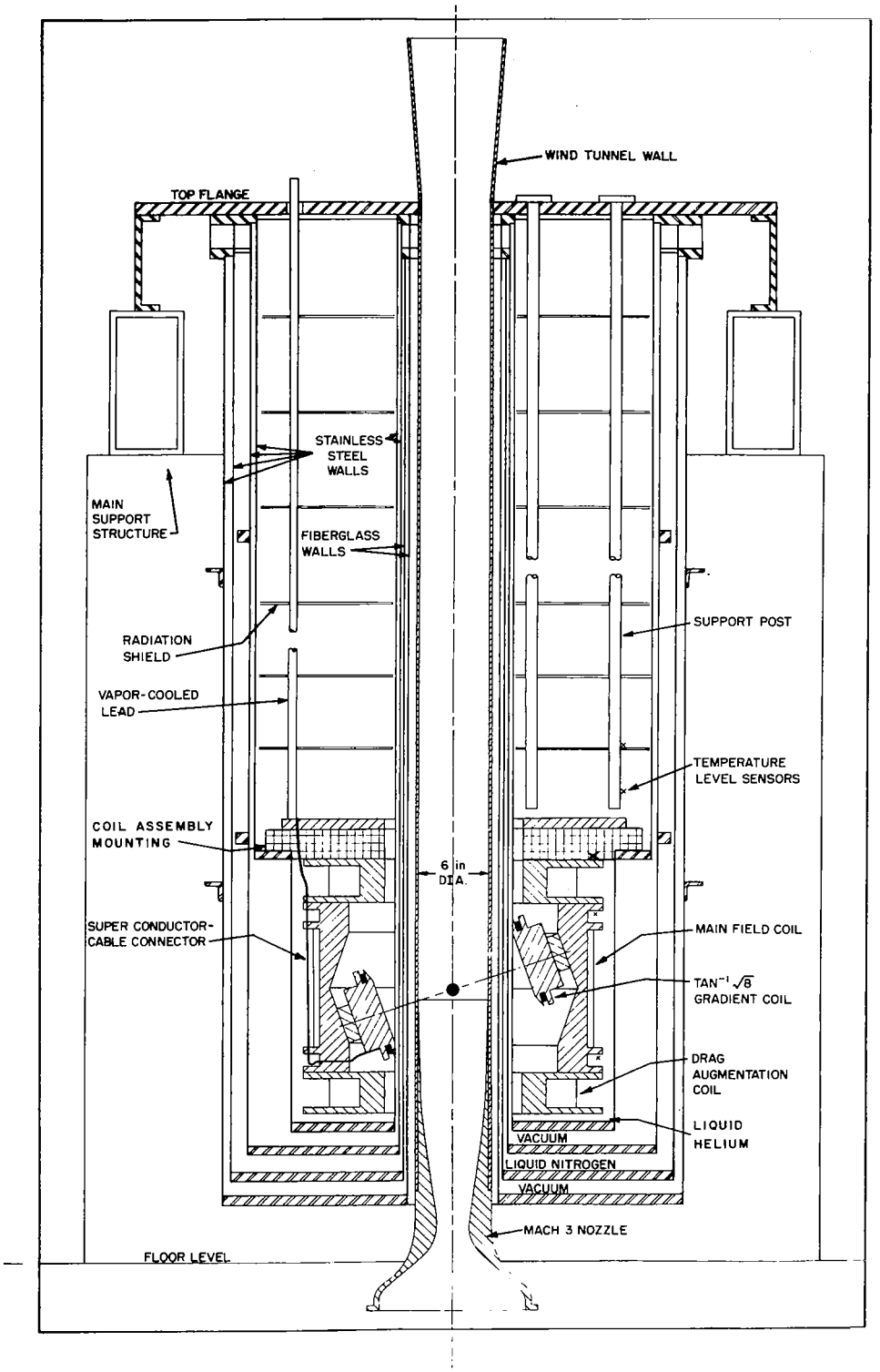

Figure 4 Sketch of Prototype Magnetic Suspension and Balance.

pressure reaches several torr. It is clear that pressure and temperature instrumentation requirements result from the need to perform the pre-cooling operation. Additional requirements result from the need to determine liquid level during liquid helium transfer and during the performance of a test.

Conventional vacuum gauges are adequate for measuring all working pressure levels between atmospheric pressure and the ultimate vacuum (about 10^{-4} torr) achieved in the jackets surrounding the nitrogen and the helium dewars. Temperature information is needed at three specific temperature levels: (1) room temperature, as a reference for the measurement of coil parameters (R,L,Q), (2) liquid nitrogen temperature, as an indicator of the state of readiness of the pre-cooling process, (3) liquid helium temperature as an indicator of coverage by liquid helium during transfer. Miniature carbon resistors are installed at five locations, marked with an x in Figure 4, between the lower surface of the bottom coil and the first radiation shield above the coil assembly. These resistors are bonded to large masses (for example, the flange of a DA coil) so as to insure that their temperature reflects that of a given part of the coil assembly rather than being dictated by local heat transfer conditions. Furthermore, their operating current is minimal. The output circuit has been arranged so as to produce calibrated readings of the three temperatures of interest at conspicuous points on the readout scale. No practical meaning is attached to readings at intermediate points.

In addition to the temperature sensors, a set of five liquid-level sensors are located at nearby locations. These are particularly useful during the balance tests as the level of liquid helium descends, but uncovered portions of the coil assembly remain at essentially liquid helium temperature. The liquid-level sensors are carbon resistors similar to the temperature sensors, but they are installed so as to be thermally isolated from large masses. Furthermore, a relatively large current is constantly circulated through them. As these sensors become uncovered their temperature rises substantially above that of liquid helium. Their output circuit uses a very effective sound alarm system as a readout.

The basic instrumentation set of the cryogenic subsystem is completed with a gas flowmeter connected in the main line of the manifold that collects the output from all vapor-cooled leads in the system. The basic function of this instrument is to provide a good indication of the total instantaneous helium boil-off rate inside the cryostat, mostly as a safety warning of coil malfunction and to measure a.c. losses.

2.3 Control System

The control system for the cryogenic magnetic suspension underwent an evolutionary process as operational experience with the facility increased. In the initial stages of development it was believed that a nonlinear controller would be necessary to maintain liquid helium boil-off within acceptable limits. This arose as a result of a study of the energy optimal controller (3) which had an open-loop control result and a compromise - the time optimal controller - which resulted in a closed-loop control and acceptable boil-off.

The nonlinear controller had operational limitations in that it was not easy to make minor adjustments to compensate for inexact system modelling and for different aerodynamic models. Therefore this approach was abandoned as experience showed that the helium boil-off rate was not as high under dynamic conditions as expected.

The nonlinear controller was replaced with a velocity plus position feedback controller. However, this was not a straight forward realization in that a Luenberger observer was utilized to obtain the velocity feedback. The additional complication of this approach (over direct differentiation of the position signal) was necessitated by noise on the position signal caused by power line ripple on the laser source for the sensor and by mechanical resonances in the structure. The primary limitations of this approach were the number of operational amplifiers required to construct the observer and, again, the difficulty of "fine tuning" the control. Therefore, when filtering and a better laser source had reduced the noise to an acceptable level, the observer was abandoned in favor of direct differentiation of the position signal. Thus the controller in use at this time, and for most of the closed-loop tests run to date, is

a linear velocity plus position feedback controller where the velocity is obtained by differentiation of the position signal. The primary advantages of this type of control are simplicity, reliability due to fewer active components, and ease of adjustment by control of velocity and position gain controls. A block diagram of the control system is shown in Figure 5. The components of the control system are discussed below.

Position Sensor: There are three requirements for model position information during a successful run of this facility. These are: (a) the operator of the facility needs to see the model for proper coordination of the launching and recapturing maneuvers, (b) an error signal is needed to close the automatic control loop effecting stable model support, (c) position and attitude coordinates, as functions of time, constitute the model "trajectory" information needed as data to compute the desired aerodynamics parameters.

The practical difficulties of establishing a direct optical path between a suspended model and an outside observer should be apparent upon re-examination of Figure 4. The many optical elements necessary to bend the light rays around the dewar become relatively inaccessible for modifications and for fine adjustments. Moreover, the annular space between the dewar and the wind tunnel, where any type of model position detector must be installed, should not be made larger than strictly necessary because as the thickness of this annulus grows so does the distance between the coils and the model (constraint (ii) in the previous section). In retrospect, it looks now that the emphasis on minimizing model-coil distance need not have dominated the design of this part of the facility. Much of the effort devoted to getting a model position sensor finally to work adequately would have been unnecessary had we increased the room temperature tubular space inside the dewar by two to three centimeters in diameter. Unfortunately, the decision concerning this initial dimension had to be made very early in the process of designing the facility and could not be changed later for obvious reasons.

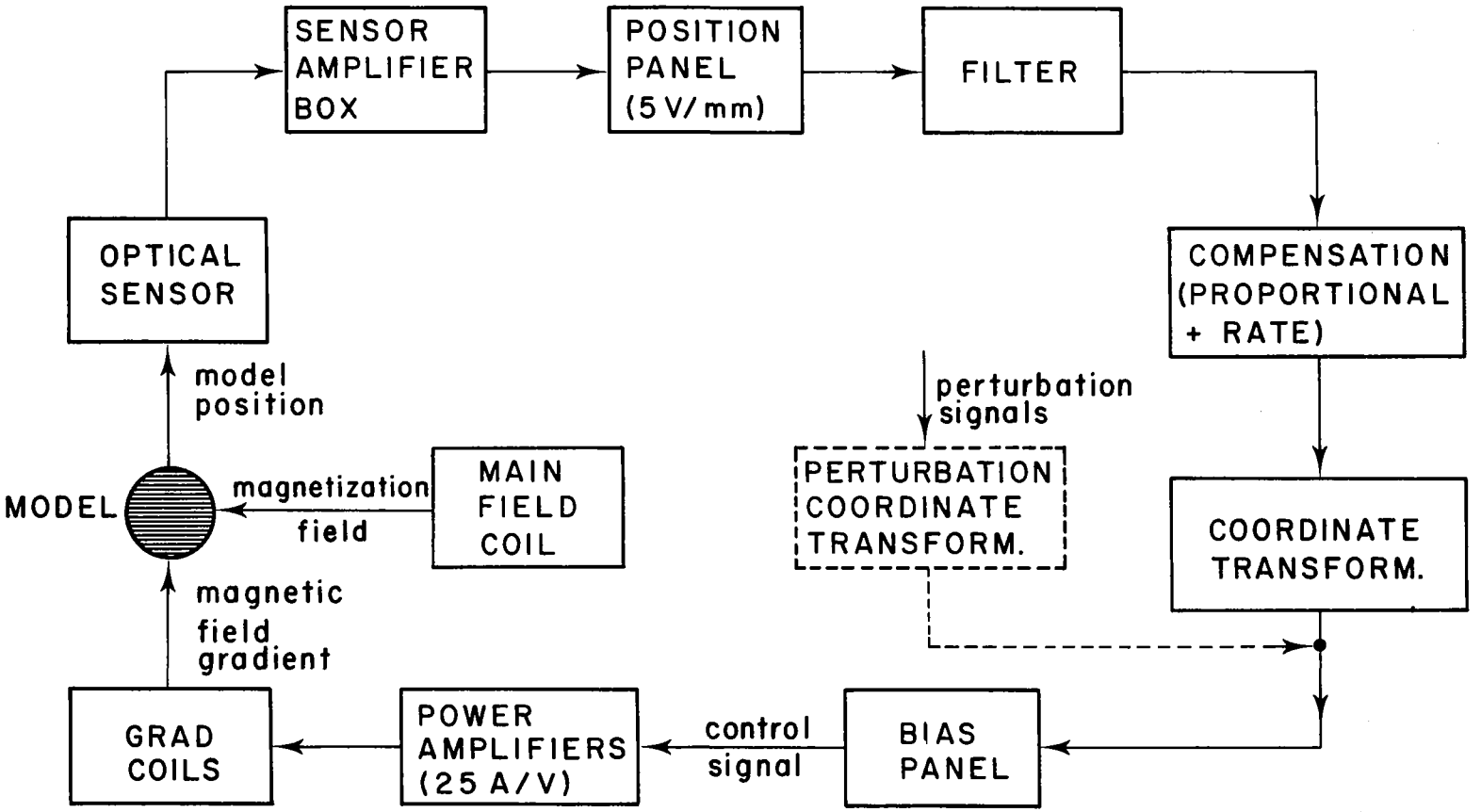

Figure 5 Block Diagram of Control System.

Requirement (a) above, has been met rather marginally by two methods. The first method consists of direct observation of the test section through a side port in the stagnation chamber of the wind tunnel via a mirror inserted on the air feed pipe. This arrangement can be seen in Figure 6. It provides a poor quality view of the model because the optical path must cross three antiturbulance screens downstream of the mirror. The second method consists of a wide-angle lens optical viewer mounted on the test section wall which utilizes narrow lenses and mirrors to provide an optical path through the annular space between the wind tunnel and the nitrogen dewar walls. This system suffers from a rather narrow field of view.

Requirements (b) and (c) demand high resolution systems. Traditionally error signals for magnetic balance control loops have been obtained from optical detectors employing different combinations of light beams, photocells, and other components. These detectors are relatively simple to operate and have built a good record of reliability. Their one important disadvantage is that they must be tailored to a given model. This inconvenience made us look with favor on the development of an electromagnetic position sensor by the MIT magnetic suspension group. This type of sensor operates on the principle of the differential transformer; its key advantages from our point of view, are: (1) one sensor can be used for different models with no modifications required, (2) the spacial distribution of the sensing elements lends itself admirably to the tight space available in our facility. Details about this potentially very attractive detector may be found in reference (6). Suffice it to say here that there are serious difficulties associated with effective utilization of this approach, mostly because of the extreme sensitivity of the device to high frequency electromagnetic signals emitted by the gradient coils as a result of the pulsating nature of the power amplifiers used (see corresponding section below). Hence, it was not possible to adopt the electromagnetic position sensor for this facility and a more or less conventional optical detector was used.

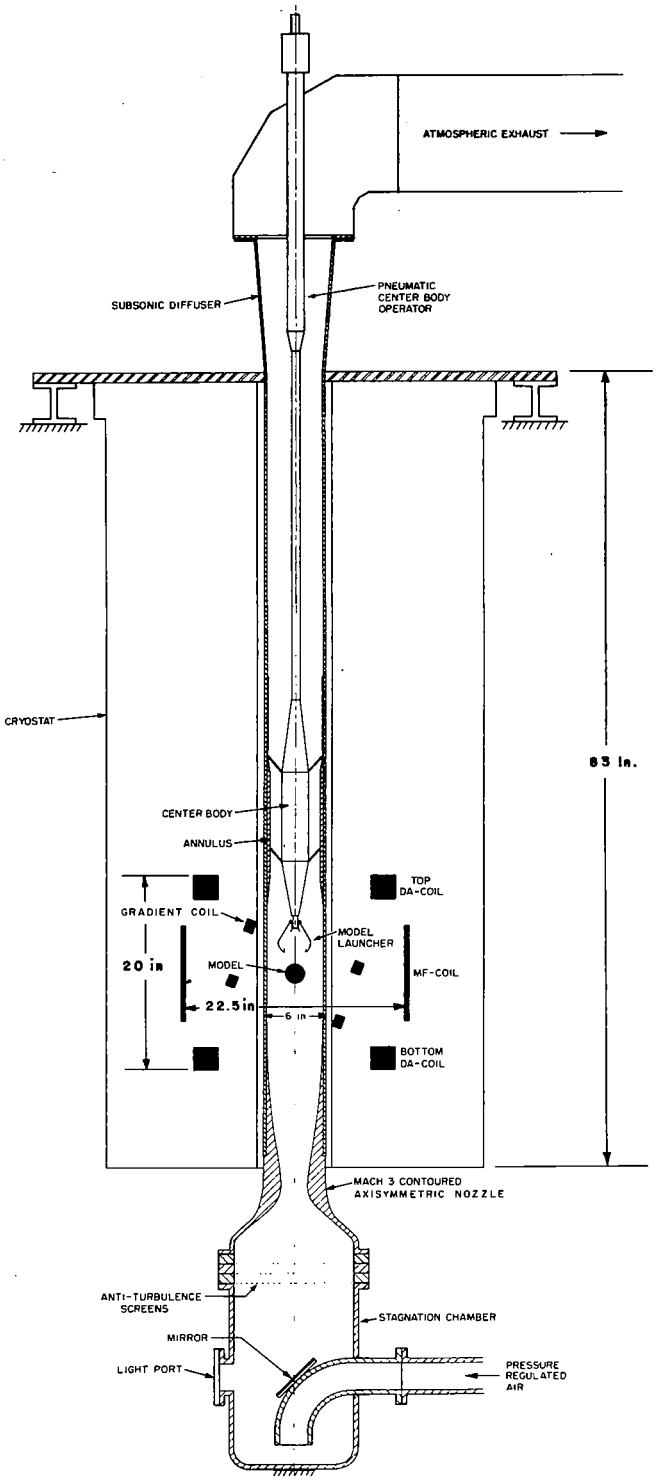

Figure 6 Overall Prototype Facility Sketch.

The optical detector consists of an optical source and beamsplitting and beamsteering optics, pairs of photodiodes, and associated electronics. The beamsplitting and beamsteering optics divide the single beam from the source into three pairs of beams which are then directed up the annulus between the outer tunnel wall and the inner dewar wall. The beams are then reflected across the tunnel. The beams are partially blocked by the model at the nominal support point; one pair at the top and bottom, one pair at each side and the third pair at each side 90° degrees from the second. As the model moves in one of the axes, the model blocks more of one beam and less of the other. The beams are then reflected down the annulus and focused onto photodiodes mounted below the bottom of the dewar. Figure 7 is a sketch of an optical sensor channel where the beam across the bottom of the model has been omitted for clarity.

The photodiodes are connected to current-to-voltage converters, and the signal for a channel is derived by subtracting the two signals of the pair. This differential configuration of the sensor eliminates much of the common mode error from source intensity variations and source noise.

The gain of each channel is adjusted to provide 5 volts per millimeter of model motion. In addition an operator's control panel is provided with meters for each channel and manual position controls which allow the operator to move the model small amounts about the nominal support point. A schematic diagram of the sensor electronics is given in Figure 8.

Filter: The filter is a standard unity-gain inverting operational amplifier low pass filter with switch selectable breakpoints of 100, 60, and 30 Hz. The correct filter for a particular model is usually chosen by perturbing the model with a square wave and observing the response.

Coordinate Transformation: As stated elsewhere in this report, the cryogenic support coils are arranged to provide a $\tan^{-1}\sqrt{8}$ system. Thus the force axes are an orthogonal set but do not provide a convenient set of axes for model measurements. The sensor that was previously

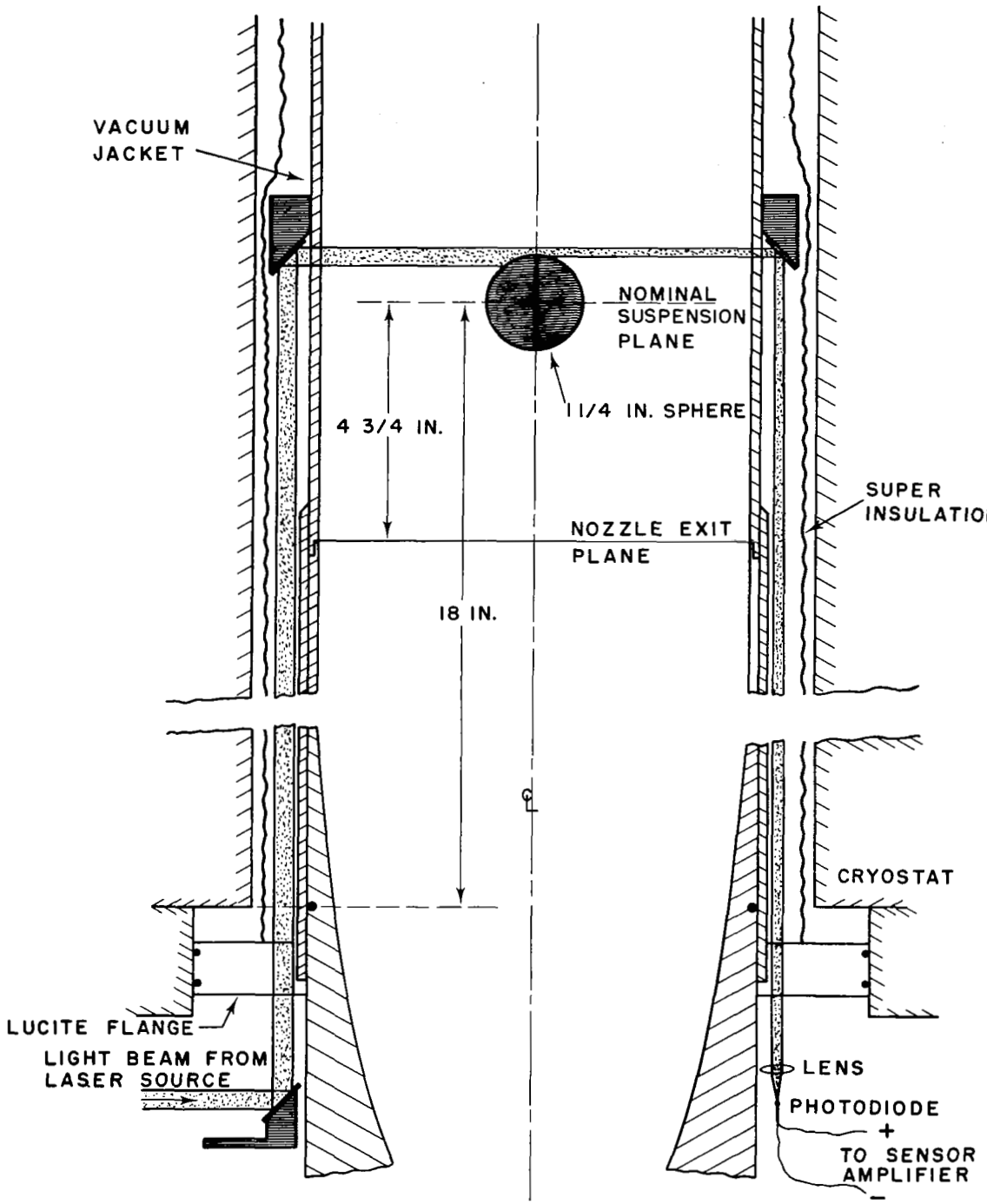

Figure 7 Optical Sensor Channel.

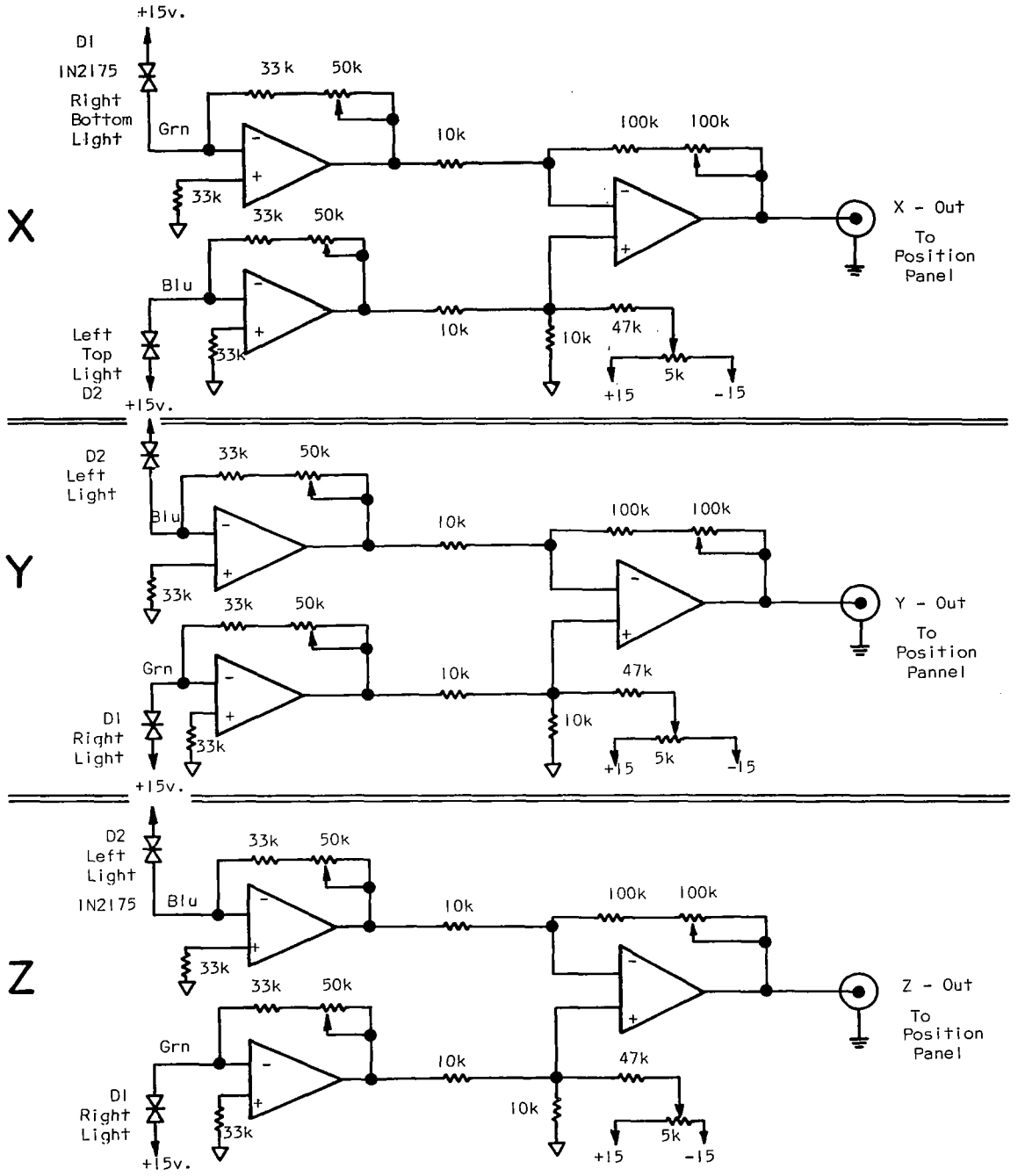

Figure 8 Schematic of Sensor Electronics.

described measures model motion along three mutually perpendicular axes with the x-axis being aligned with the tunnel axis (vertical). Therefore a transformation from the tunnel coordinate system to the $\tan^{-1}\sqrt{8}$ system is needed. If the tunnel axes are designated by x,y, and z and the $\tan^{-1}\sqrt{8}$ axes are designated by x', y', and z', then the transformation is given by

$$\begin{pmatrix} x' \\ y' \\ z' \end{pmatrix} = \begin{pmatrix} \frac{\sqrt{3}}{3} & \frac{\sqrt{3}}{3} & \frac{\sqrt{3}}{3} \\ \frac{\sqrt{3}}{3} & -\frac{\sqrt{3}+1}{2\sqrt{3}} & \frac{\sqrt{3}-1}{2\sqrt{3}} \\ \frac{\sqrt{3}}{3} & \frac{\sqrt{3}-1}{2\sqrt{3}} & -\frac{\sqrt{3}+1}{2\sqrt{3}} \end{pmatrix} \begin{pmatrix} x \\ y \\ z \end{pmatrix}$$

Thus the three sensor signals are transformed into equivalent motions in the coil coordinate system. This transformation is realized as shown by the schematic diagram in Figure 9.

This circuit was duplicated as shown in the block diagram of Figure 5 to facilitate the input of model perturbations in the tunnel coordinate system. The perturbation signals are applied after the system compensation to avoid the frequency response shaping.

Bias Panel: The power amplifiers which drive the gradient coils require approximately -7 volts for minimum current and +7 volts for maximum current. Therefore a bias voltage is inserted into the control loop to set the nominal support current. This is an operational amplifier circuit in which the bias is algebraically added to the control signal.

Power Amplifiers: The power amplifiers which drive the three pairs of gradient coils were built to specifications provided by the University of Virginia. A summary of the specifications is presented in Table 2.

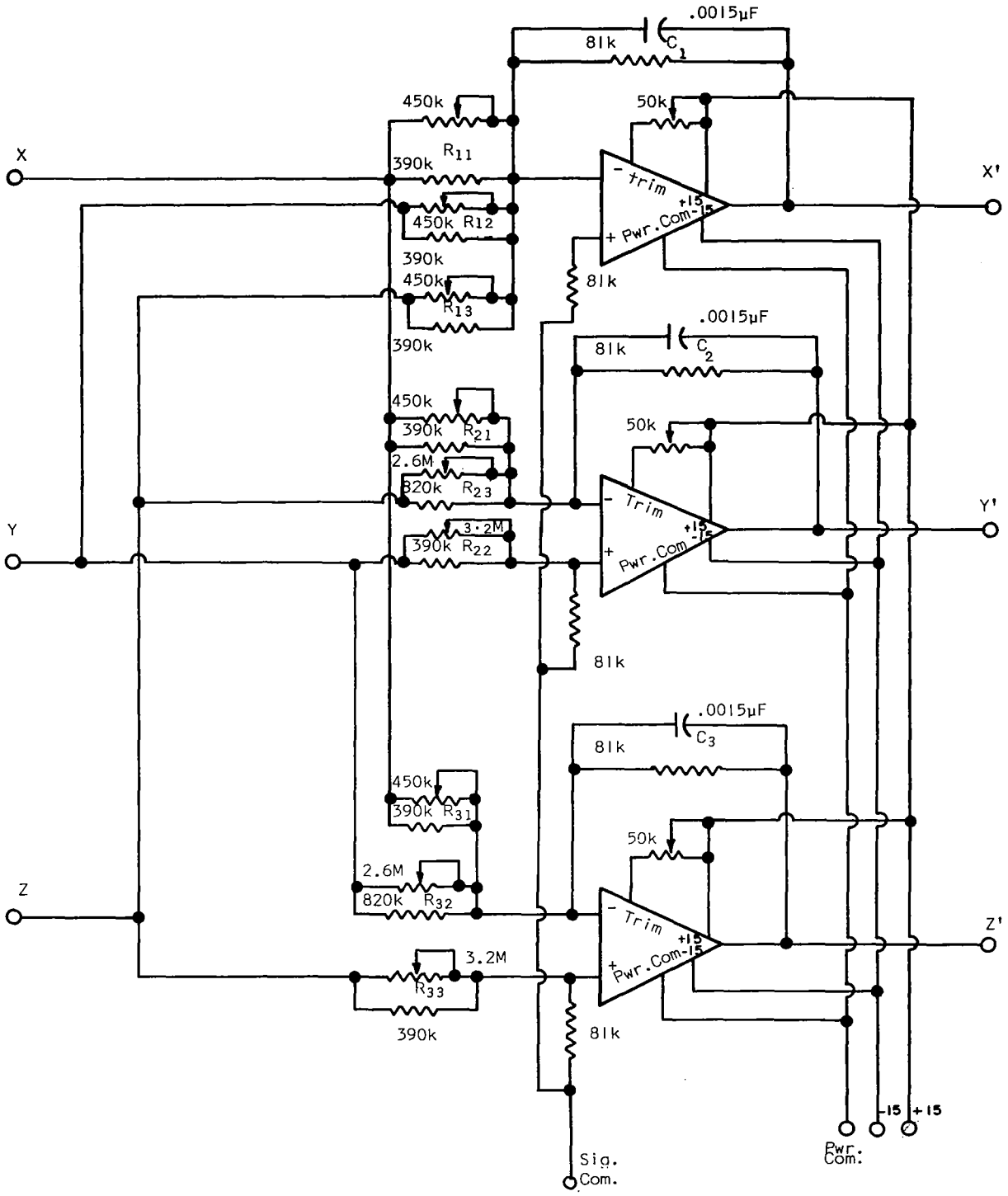

Figure 9 Schematic of Coordinate Transformation.

TABLE 2

POWER AMPLIFIER SPECIFICATIONS

Supply Voltage (Complete Plant)	3 X 440 V 60 Hz
Value of Regulated d.c.	210 V
Input Voltage (Signal)	-7 to +7 V
Output Current	10 to 350 A
Time for Current Rise 10-350A	16 MSEC. MAX.
Current Ripple at Constant Current	± 9 A
Load Resistance	60 mohm MAX.
Load Inductance	8 mH ± 5%

The power amplifiers are switching type amplifiers with force-commutated thyristors as the switching elements. The power amplifiers are usable to almost 300 Hz. After almost four years of use they have proven to be quite reliable. This is to a large extent due to the many protective features that were provided. Thus, the power amplifiers are automatically switched off in the event of

1) Failure of input power or any of the phases
2) Failure of cooling water flow
3) Failure of any of the several cooling fans
4) Failure of fuses in commutation or load sections
5) Overload of the input rectifier
6) Application of +10 volts to the emergency input
7) Actuation of door interlocks.

The power amplifiers were designed for a run time of 10 minutes at highest-frequency highest-current conditions with a 30 minute rest between runs. However, runs under significantly less stringent conditions typically are 15 minutes with 10-15 minute rests.

Compensation: This part of the control system has received the most attention during the development of the cryogenic support system. As stated in the introduction the final approach to compensation is largely

the result of operational experience gained over several years. In order to explain some of the difficulties encountered and, hopefully, to aid others in similar endeavors, a brief discussion of the approach is in order.

Because of the fact that a support system of this type is inherently open-loop unstable, it is practically impossible to compensate the system by purely "cut and try" methods. Thus in order to even take realistic experimental data, the system must be made closed-loop stable by some means. To further complicate the process, it costs approximately 1,000 dollars in liquid helium alone for two days operation. Thus the amount of time available to experiment with the system dynamics was severely limited. To alleviate this latter problem, a scaled down water-cooled coil system was constructed which would accommodate the actual position sensor. This water-cooled system would not support the model vertically, but horizontal support could be achieved by suspending the model from a string. By taking into account the difference in force constants between the cryogenic and water-cooled coil systems, experimental data for the cryogenic balance could be extrapolated. This technique saved a considerable amount of time and money.

A compensation network for each channel was designed using the theoretical values of the system constants and a theoretical model for the system dynamics. This network was a velocity (or rate) plus position network where the velocity was obtained by differentiation of the position sensor signal as shown in Figure 10. This network was inserted into the loop as shown in Figure 5, and the control system was connected to the water-cooled coils. The operation was satisfactory with only minor adjustment of the gain controls.

The system was checked by injecting an adjustable frequency sine wave into the perturbation input and measuring the response at the sensor output. The results agreed closely with the theoretical model.

This same compensation (with different gain settings to account for different force constants) was then tried on the cryogenic system with somewhat less satisfactory results. Stable three-dimensional support

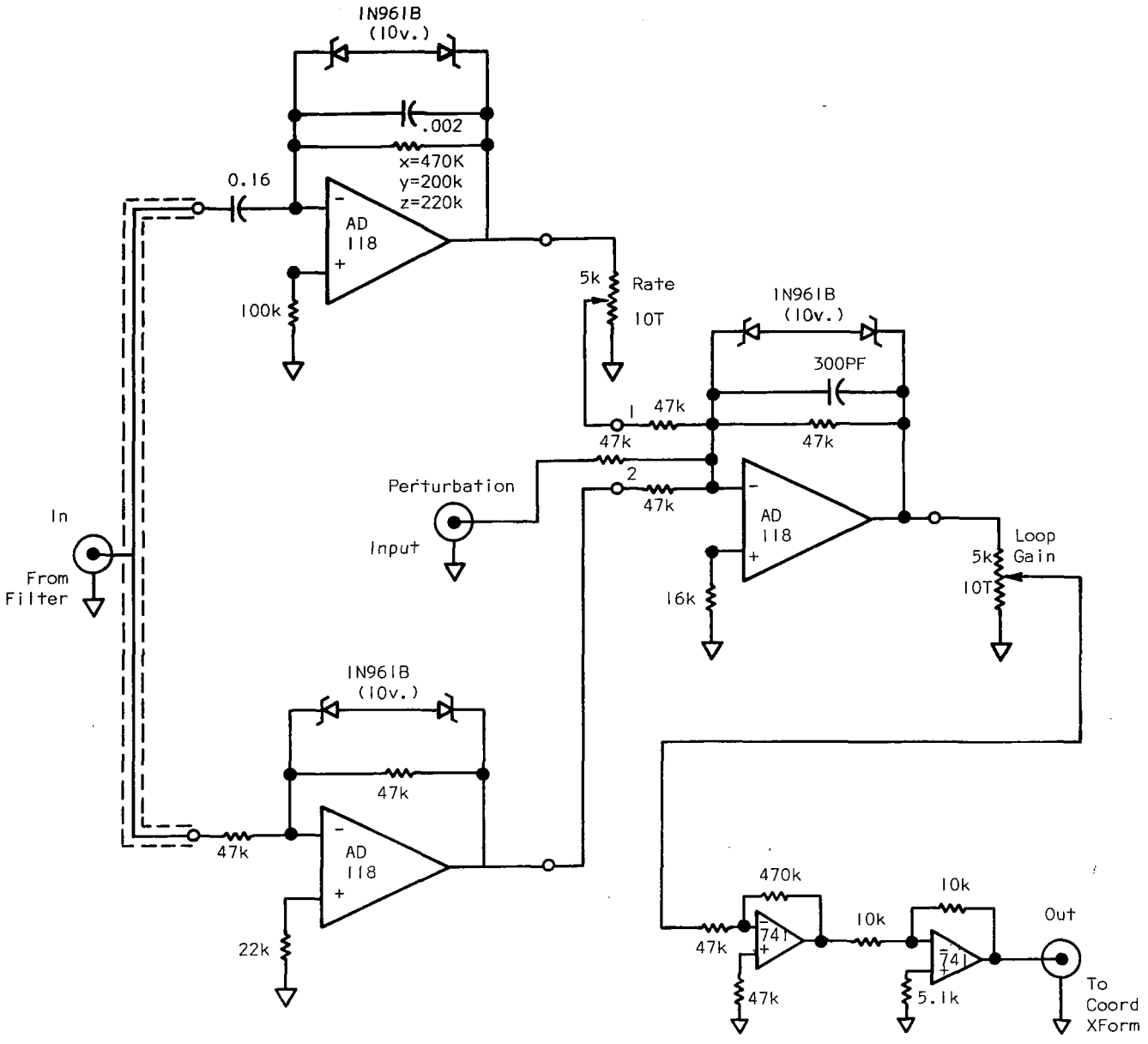

Figure 10 · Schematic of Compensation Circuit.

could be achieved at low values of main field magnetization, but as the magnetization was increased, the model would drift toward the tunnel wall until support was lost. Furthermore dynamic testing as explained above showed unaccountable low-frequency (less than 10 Hz) resonances. The former problem was corrected by more precise alignment of the sensor nominal support point with that of the coil system. The latter problem was corrected by stiffening the dewar mounting and eliminating the pendulum mounting of the coil structure. After these changes were made the support was operated to design values of main field current.

2.4 D.C. Power Supplies: The magnetizing or Main Field coil and the pair of drag augmentation coils have substantially different operating requirements from the gradient coils. Both types of coils are designed for open-loop current adjustment and require much smaller and simpler power supplies than those required by the gradient coils. The Main Field coil must be energized with a constant-current power supply to maintain a steady magnetizing field. Modest voltage capability is required to overcome lead and connection voltage drops and to charge the coil to rated current (nominally, 100 A) in a reasonable length of time (typically, of the order of one minute), by manual operation. These requirements, plus normal reliability and economy criteria, are satisfied by a constant-current saturable reactor type power supply, which employs no active devices other than solid state rectifiers. Current control is effected by an adjustable autotransformer making the power supply reliable and rugged.

A very important consideration in the design of the main field circuit is the amount of energy stored in the coil at rated current:

$$W = 1/2\ LI^2 = 2.55 \times 10^4 \text{ Joules}$$

In the event of a failure in some part of the circuit tending to stop or drastically decrease the current, the reverse voltage applied by the coil, if not controlled, could damage the coil and the power supply. The resulting helium boil-off is a potential safety hazard not to be taken lightly. To prevent the sudden release of energy a high-current

silicon rectifier has been connected (reverse biased normally) across the coil terminals outside the dewar. This prevents the reverse voltage from exceeding the diode drop (about 1 Volt). Furthermore, this diode and its lead resistance permit a faster shutdown of the Main Field coil under normal operating conditions.

In as much as the function of the Drag Augmentation coil is to balance the steady-state component of the aerodynamic drag minus the model weight, the operational mode for these coils must be described as slowly adjustable d.c., with an anticipated response-time requirement on the order of a few seconds. This operational capability, permitting the average Gradient coil current to remain at a steady level for maximum range, can be achieved with a voltage-controlled current source. The model vertical position sensor and proper compensation comprise the remainder of the drag-augmentation control loop.

A voltage-controlled current source (0-64 VDC, 0-150A), with provision for manual or remote programming was chosen. The upper voltage limit of 64 volts is capable of producing a response on the order of:

$$\Delta t = L\Delta i/E_{max} = 20 \text{ seconds}$$

for a current change of 0 to 100 A through the combined inductance of 12.4 henries of the DA coil pair. A reverse silicon diode across the terminals was installed as a safety protection against sudden decreases in coil current, for reasons similar to those discussed in the previous sub-section.

2.5 Supersonic Tunnel: The wind tunnel is a Mach 3 blow down facility with atmospheric exhaust. The circular test section is 14.6 cm in diameter. Air is stored at 18 atmospheres in two 28 m^3 tanks enabling the facility to run for about 4 minutes at 3.25 atmospheres stagnation pressure with a run cycle of 90 minutes. To increase run time and decrease aerodynamic loads on the suspended models an optimized variable second throat arrangement is employed, which permits tunnel operation at 3 atm stagnation pressure with a 1 in. spherical model.

Figure 6 is a sketch of the facility which illustrates the relative size and location of wind tunnel components vis-a-vis magnetic suspension components.

Axisymmetric tunnels have well known problems with flow non-uniformities which tend to "focus" in specific test section locations. Our tunnel is no exception and flow quality improvement has been a slow and difficult process which is still in progress. This difficulty is particularly troublesome in connection with aerodynamic testing of slender bodies (e.g. conical or power law shapes). Work on this problem is continuing under separate sponsorship and will be reported in detail in the open literature when completed.

3. OPERATIONAL CHARACTERISTICS

The superconductor magnetic suspension and balance prototype facility has unique operational characteristics stemming from the particular coil configuration used, from the superconductor nature of the magnetic coils, and from the type of wind tunnel used. Different relevant aspects of the operation of this facility are discussed in separate sections below.

3.1 Static Force Calibration: One of the principal advantages claimed for the coil configuration adopted for this facility is the linearity of the relationships between the magnitudes of support coil currents and magnetic forces exerted on supported models. This characteristic makes the magnetic suspension an attractive wind tunnel balance (a 3-component balance in this particular case). In the most general case, all three types of coils in the prototype configuration can exert forces on a magnetized model. In the sketch of Figure 11, the ferromagnetic sphere is shown suspended a distance $+\Delta x$ above the nominal suspension point. Hence, for small Δx (6):

$$F_{MAG,x} = F_{DA} + F_{MF} + F_{GRAD}$$

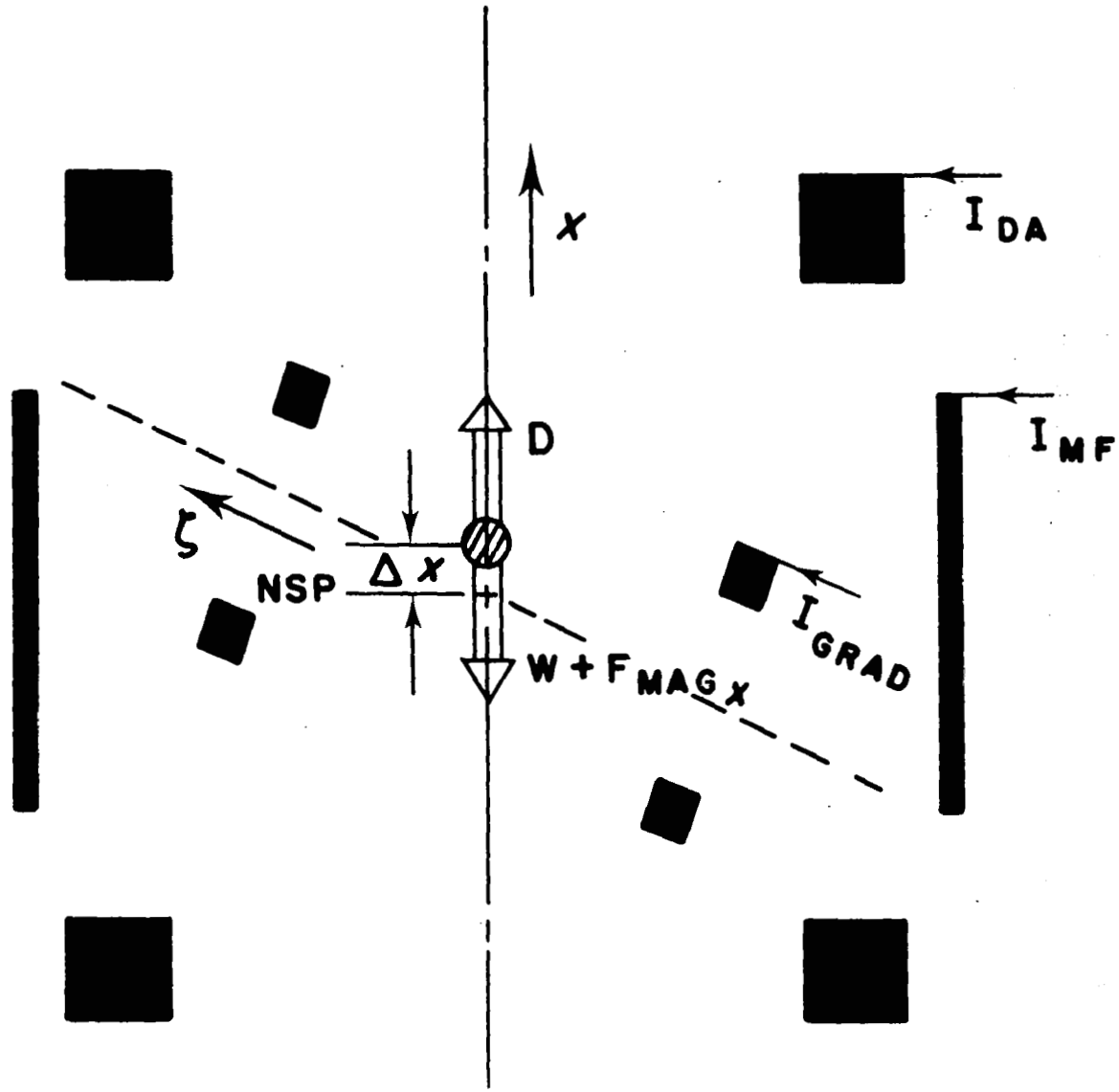

Figure 11 Vertical-force development.

$$= \mu_o MV \left(\left(\frac{\partial B_x}{\partial x} \right)_{NSP,DA} + \Delta x \left(\frac{\partial^2 B_x}{\partial x^2} \right)_{NSP,MF} + k \left(\frac{\partial B_\zeta}{\partial \zeta} \right)_{NSP,GRAD} \right)$$

$$= \alpha W I_{MF} I_{DA} + \beta \Delta x W I_{MF}^2 + \gamma W I_{MF} \sum I_{GRAD},$$

where F represents force, M is the intrinsic magnetic moment per unit volume induced in the sphere by the main field, V is the sphere volume, B represents magnetic induction, x and ζ are axial coordinates (see Figure 11), W is the sphere weight, I represents electric current and α, β, and γ are constants for a fixed geometric coil configuration, and where it has been assumed that the model magnetization increases linearly with main field current I_{MF}. Note that, to a first order approximation, there is a vertical force exerted on the model by the magnetization coil which is proportional to the magnitude of the vertical misalignment of the model with respect to the nominal suspension point. Note also that, in general, all three gradient coil pairs contribute to the vertical force linearly. Finally, it is worth noting that the above force equation is basically a vector equation, i.e., the directions of the contributions of the drag augmentation coils and the gradient coils depend on the directions of current flow through such coils (or coil magnetic polarities) with respect to the current flow (or polarity) of the main field coil. Vertical displacement of the model always produces a force in a direction opposite to the displacement.

The magnitudes of the constants α, $\beta\Delta x$, and γ were determined by a detailed calibration of the magnetic balance in which a 3.17 cm model was suspended by a string from a load cell (simulating the drag force on the model) and stabilized laterally near the nominal suspension point by the magnetic suspension. Main Field current was used as a parameter while drag augmentation current was varied over a wide range of values for the two polarities of the gradient coils relative to that of the main field coil. Results are summarized graphically in Figure 12. Linearity is excellent throughout. Constants α and γ have experimental uncertainties of less than 1 and 5% respectively. The much larger uncertainty associated with the determination of $\beta\Delta x$ is undoubtly due to insufficient care in holding Δx constant from one experiment to the next.

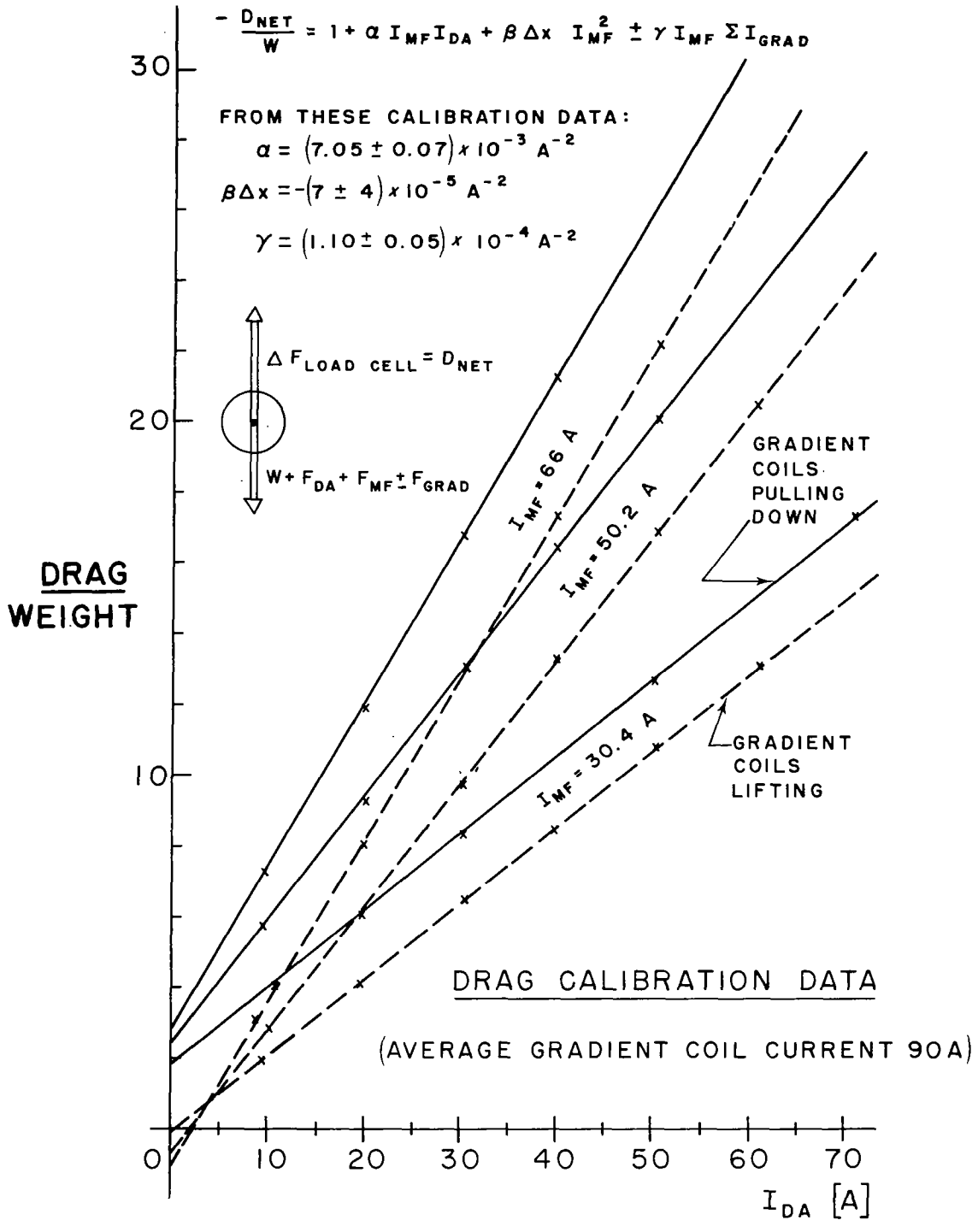

Figure 12 Drag Force Calibration Results

However, this should present no serious practical problems in actual operation for two reasons: First, the magnitude of the contribution of the main field coil to the overall vertical force is small compared to the contributions by drag augmentation and gradient coils for values of D/W in the range of operating conditions for supersonic flow. Second, by careful adjustment of optical sensor components, Δx can be made arbitrarily small and thus, F_{MF} can be made vanishingly small even for moderate and low D/W situations.

Based on the above calibration results, the range of drag augmentation and main field current settings necessary for supporting a 3.17 cm sphere in Mach 3, 3.25 atm stagnation pressure air flow have been computed and are listed in Table 3. Note that the average magnitude of the current in each gradient coil pair has been assumed at midrange, i.e., 175 A for a total of 525 A for all three pairs.

TABLE 3

Current Settings for Mach 3, 3.25 atm Flow
$(D-W)/W = 33.86$, Assuming $C_D = 1$, $d_{SPHERE} = 3.17$ cm

I_{MF}(A)	$\gamma\ I_{MF} \sum I_{GRAD}$	needed $\alpha\ I_{MF} I_{DA}$	needed I_{DA}(A)
60	3.21	30.66	78.2
65	3.48	30.39	71.6
70	3.75	30.12	65.9
75	4.02	29.85	60.9
80	4.28	29.59	56.6

3.2 Dynamic Response

As stated in section 2.3, the design of the control system for this magnetic suspension underwent an evolutionary process as operational experience with the facility increased. Thus it is somewhat artificial to separate the description of this control system into design and operational aspects. Nevertheless, to follow the order of presentation adopted for this report, dynamic response measurements are mentioned here. These measurements were performed for all three tunnel axes using sine wave perturbation in closed loop mode. Results for one of the horizontal axes are shown in Figure 13. Figure 14 shows results for the vertical axis.

3.3 Cryogenic Performance

Time, cost, and safety are the principal aspects of the operation of this prototype facility which are directly related to the use of superconductor technology to implement the coil system.

Time is a significant parameter both before and during aerodynamic testing. A precooling period of about 36 hours is necessary to prepare the facility for economic liquid helium transfer (about 800-1000 liters of liquid nitrogen are used for precooling). Normally it takes about 4 hours between liquid helium transfer starts and the first experiment can be run. From this point, about 8 hours of run time are available before additional helium has to be transferred. A two-day experiment will consume between 400 and 500 liters of liquid helium and yield between 12 and 16 hours of useful run time. With the available air storage-wind tunnel combination a maximum of 10 4-minute runs at Mach 3 can be accomodated in this period. It should be apparent that better-than-usual experiment planning is required for economic utilization of the facility.

The principal operational cost is due to the consumption of cryogenic fluids. Using the figures given in the preceeding paragraph and assuming unit costs of \$0.23/ℓ for liquid nitrogen and \$2.05/ℓ for for liquid helium plus \$100 for transportation expenses for liquid

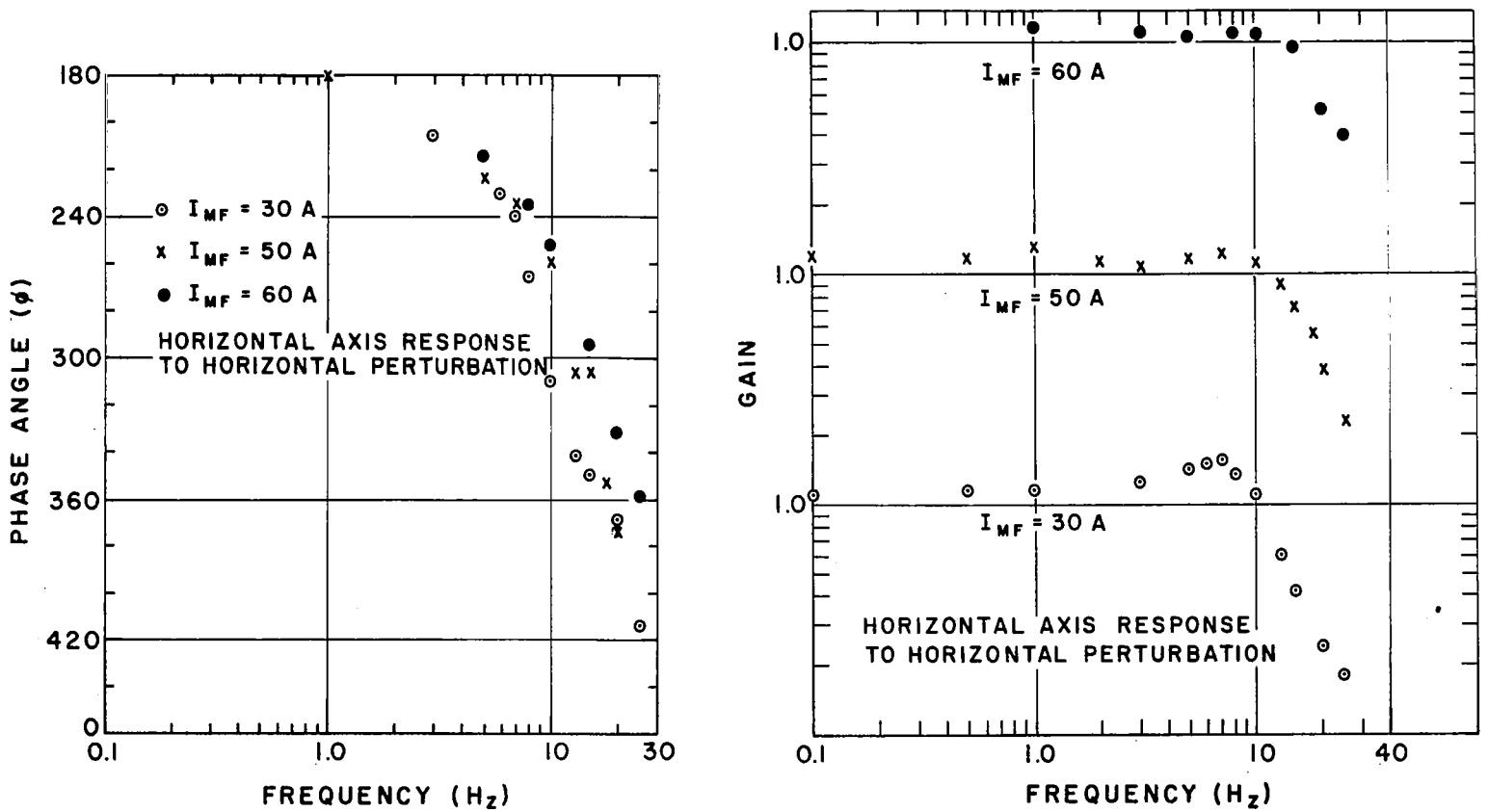

Figure 13 System Dynamic Response: Horizontal Axis.

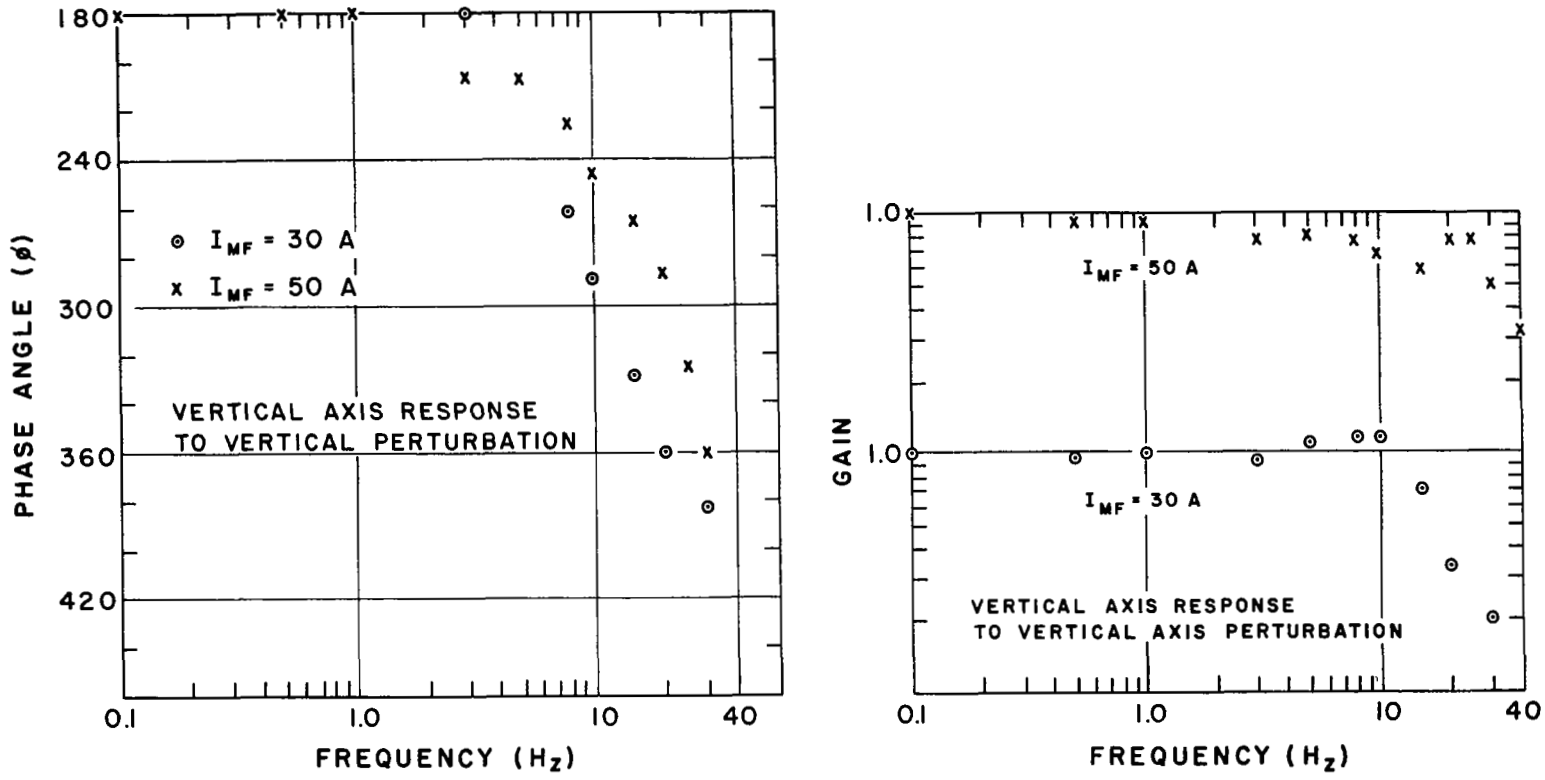

Figure 14 System Dynamic Response: Vertical Axis.

helium, a two-day experiment costs between $1,100 and $1,300, or an average of $120 per 4-minute run.

To put the above cost estimates into proper perspective it should be kept in mind that this prototype facility is by no means optimum from the viewpoint of cryogenic fluid consumption. It must be remembered that at the start of this project there were strong doubts among applied superconductivity experts concerning the feasibility of operating superconductor coils in the tightly coupled dynamic environment typical of magnetic suspension systems. The key question concerned the level of energy dissipation by the coils resulting perhaps in unacceptable helium boil-off rates or even loss of superconductivity properties in extreme cases. Now that this key question has been resolved probably a logical next step is to look into possible ways of minimizing cryogenic fluid consumption.

Several examples of liquid helium dissipation rates for different experimental situations are shown in Figure 15. Pursuing the point made in the preceeding paragraph, it should be noted that the nature of the gradient coil power amplifiers coupled with the overall complexity of the control circuit in the prototype facility results in a relatively large high frequency content in the gradient coil currents. Thus results shown in Figure 15 represent a worse case which can be improved by appropriate filtering and other control circuit refinements.

Finally, safety has been given considerable attention throughout the development of this facility which, because of its unique character involves higher-than-ordinary potential safety hazards. The combination of large quantities of liquid helium and high energies stored in the magnetic field is awesome. In response to this inherent risk, all energy sources have been protected against sudden release of this magnetic field energy into the cryostat. This was discussed in some detail in the section on Power Supplies. During runs, liquid helium evaporation rate is monitored at all times and liquid level is checked directly before every series of experiments.

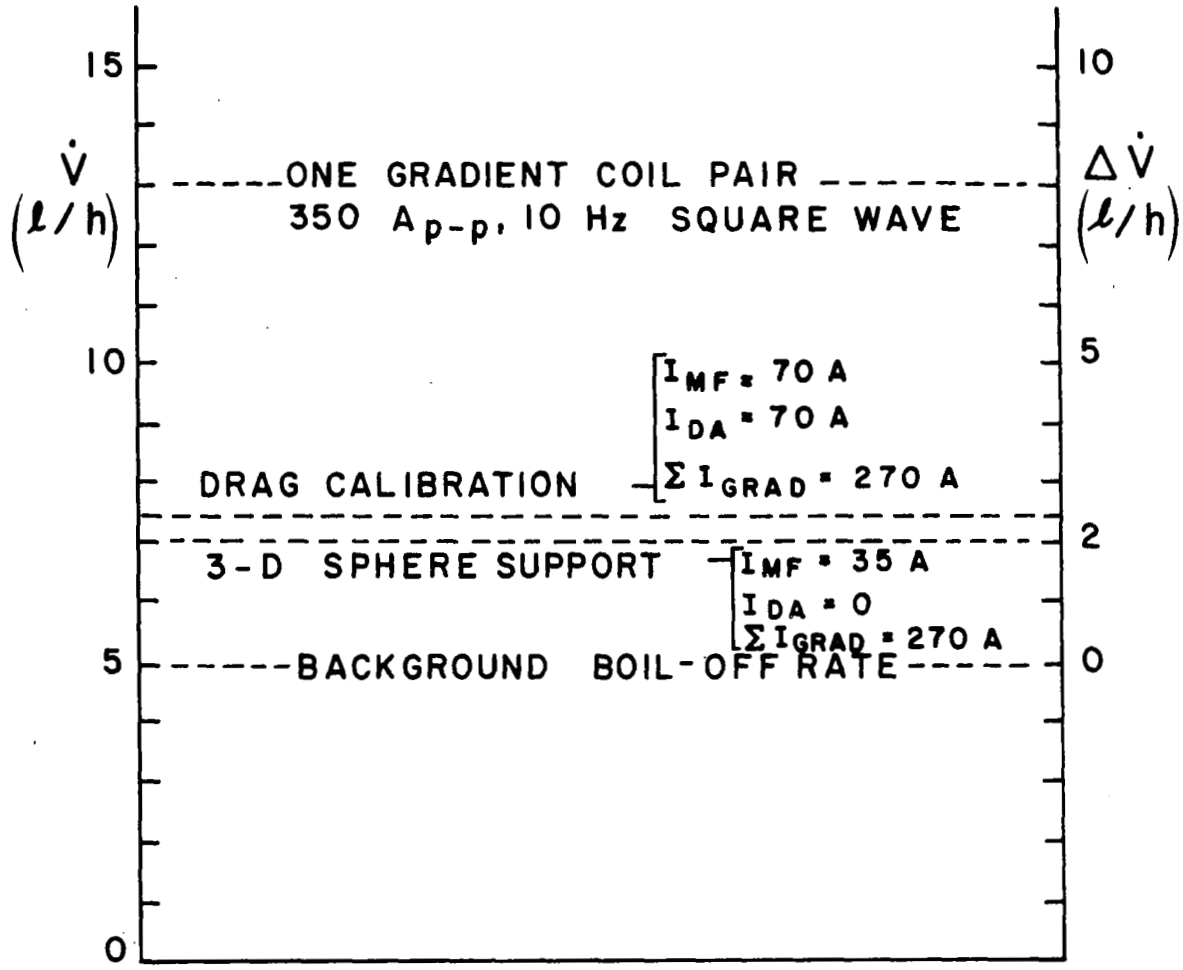

Figure 15 Typical Helium Boil-Off Rates.

3.4 Overall Energy Consumption

Although energy dissipation resulting in helium boil-off is undoubtly the principal item of energy consumption in a facility such as the one described herein, it is of interest to establish the magnitude of the total energy consumed by the facility for economic and conservation reasons. In this case the only other item of significance is the energy consumed by the power supply feeding the gradient coil power amplifiers (power supplies feeding d.c.-operated coils consume negligible amounts of energy, corresponding to power dissipation in the leads). Direct measurements of power dissipation in the gradient coil power supply have not been made. However, a reasonable estimate can be made based on upper limits determined by the main fuses of the power amplifiers. This yields an upper limit of 18 kwatt per power amplifier. This rate of dissipation could conceivably be achieved by operation at maximum current (0-350 A) and maximum frequency (may be 100 Hz) over the entire experiment. It is estimated that, on the average, only about 20 to 30 percent of this maximum power is used. Hence, the total power dissipation from this source is about 10 kwatt. Assuming 10 runs of 4 minutes each, we get 13.5 kwatt-hour dissipation in a two-day experiment.

Cryogenic fluid consumption can be converted to equivalent kwatt-hours by estimating the power needed to produce liquid helium and liquid nitrogen. The following conversion factors are used:

6.2 kwatt-hour/ℓ L He

0.8 kwatt-hour/ℓ L N_2

Since we estimated consumption at 500 liters of helium and 1000 liters of nitrogen, the grand total is as follows:

Helium	6.2 x 500	=	3,100 kw-h
Nitrogen	0.8 x 1000	=	800 kw-h
Power amplifiers			14 kw-h
Total energy per experiment			3,914 kw-h

3.5 Aerodynamic Testing Performance

Two types of aerodynamic models, spheres and cones, have been successfully suspended in the prototype facility. Most of the tests have been wind-off to determine the operating characteristics of the suspension system. It was explained in section 2.5 that the axisymmetric supersonic wind tunnel has been plagued by flow irregularities which have proven difficult to eliminate. As a consequence, no reliable supersonic aerodynamic data are available to date. The development of this prototype facility followed a course such that the emphasis was shifted heavily towards the proof of the concept of a superconductor magnetic suspension at the expense of emphasis on aerodynamic research capability. Hence, an extremely modest offering is presented by way of current representative aerodynamic data, namely, a measurement of sphere drag at very low flow speed. Measurements such as this were made by using the wind tunnel in a subsonic mode utilizing a simple turbine blower to move the air flow. Results are summarized in Table 4 below. The only purpose in showing this result is that of confirming the potential effectiveness of this experimental approach to aerodynamic testing.

TABLE 4

Summary of Subsonic Sphere Drag Measurement

Stagnation pressure	1 atm
Dynamic pressure	0.00145 atm (1.5 cm H_2O)
Sphere diamenter, d	3.17 cm
Reynolds number based on d	3.3×10^4
Mach number	0.045
Measured D/W	0.045
Computed value of C_D	0.48
Commonly accepted value (7)	0.47

4. SCALING TO LARGER FACILITIES

By way of introduction to the topic of scaling magnetic suspension devices for larger aerodynamic testing facilities, it should be remembered that electromagnetic suspension techniques have been applied to support models in wind tunnels for nearly twenty years. Several facilities using a variety of magnet configurations have been developed in this country and in Europe and they have made possible significant contributions to studies of a broad spectrum of aerodynamic phenomena (8). However, for all its apparent potential, the use of this valuable experimental tool has not spread as widely as originally anticipated and we are convinced that the main reason is the difficulty of building large magnetic suspension facilities. Not one of the existing facilities can accommodate a tunnel test section with a characteristic dimension larger than about 30 cm. The explanation for this limitation is simple once one considers the laws governing the scaling of magnets. These laws are discussed in the following section. Furthermore, in ordinary wind tunnels realistic Reynolds number simulation is accompanied by large aerodynamic loads (typically, large values of dynamic pressure, q). This, of course, tends to increase the demand for larger and more powerful support coils. Recent developments of the cryogenic wind tunnel concept have involved this situation greatly as discussed in section 4.3.

4.1 Scaling Laws

In 1966 Parker formulated simple scaling laws for air core magnets (1). These are summarized in Figure 16. Parameters relevant to the design of both magnetizing and gradient coils are included. From these scaling laws, Parker concluded that the most promising approach to applying magnetic suspension techniques to large facilities consisted of using magnets built of low resistivity conductors. This realization led to the "cold balance" concept, initially conceived around high purity conductors operated at extremely low temperatures (supercooled) and subsequently evolving towards the utilization of superconductors.

When superconductors are used, such as in the facility described in this report, joulian power dissipation has no real meaning since

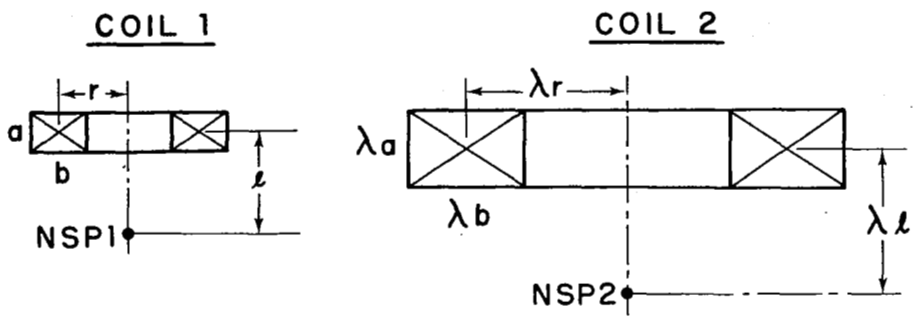

COIL	1	2
CONDUCTOR RESISTIVITY	ρ_1	ρ_2
CURRENT DENSITY	J1	J2

AT NOMINAL SUSPENSION POINT (NSP):

MAGNETIC FIELD $\frac{B2}{B1} = \left(\frac{J2}{J1}\right)\lambda$

MAGNETIC FIELD GRADIENT $\frac{\nabla B2}{\nabla B1} = \frac{J2}{J1}$

COIL VOLUME, WEIGHT* $\frac{V2}{V1} = \frac{W2}{W1} = \lambda^3$

JOULIAN POWER DISSIPATION $\frac{P2}{P1} = \left(\frac{J2}{J1}\right)^2 \left(\frac{\rho_2}{\rho_1}\right) \lambda^3$

AMPERE x TURNS $\frac{NI2}{NI1} = \left(\frac{J2}{J1}\right) \lambda^2$

*assume equal coil densities, packing factors.

Figure 16 Air-Core Coil Scaling Laws.

superconductors dissipate no power when operated in a d.c. mode. The revelant corresponding quantity is the a.c. power dissipation of the gradient coils as discussed above in section 3.3. The scaling of these power losses is not as simple as is that for conventional magnets. Experimental results reported in reference 9 point towards an a.c.-losses relationship of the form:

$$\frac{E}{f \times \ell} \sim I^{\delta}$$

where E is the rate of energy dissipation measured in terms of helium evaporation rate, f is the frequency of the sinusoidal coil excitation, ℓ is the total length of superconductor in the windings, I is the r.m.s. magnitude of the excitation, and δ has a value typically between 2.0 and 2.5. Experiments performed in our laboratory confirm this type of relationship in general as shown by results plotted in Figure 17.

In the design extrapolations discussed below it has been assumed that current magnitudes and frequencies will be the same for larger facilities as they are for the prototype facility, such that coil size and windings cross section are the only variables available to the designer. This is perhaps an unnecessarily conservative assumption since, for example, there is good reason to expect substantially lower characteristic operating frequencies in larger facilities. Also, somewhat more complicated trade-off calculations would in all probability yield more favorable combinations of sizes and current levels for gradient coils. However, given the intent of the present preliminary design calculations it makes sense to take this worst-case approach as a safety factor.

4.2 Optimized Coil Configuration

The main purpose of this design extrapolation exercise was to estimate conservatively the order of magnitude of coil size and liquid helium consumption requirements for large scale aerodynamic test facilities. Furthermore, it is useful to explore the advantages of combining a superconductor magnetic suspension and balance with a cryogenic wind tunnel. It must be pointed out, however, that no specific

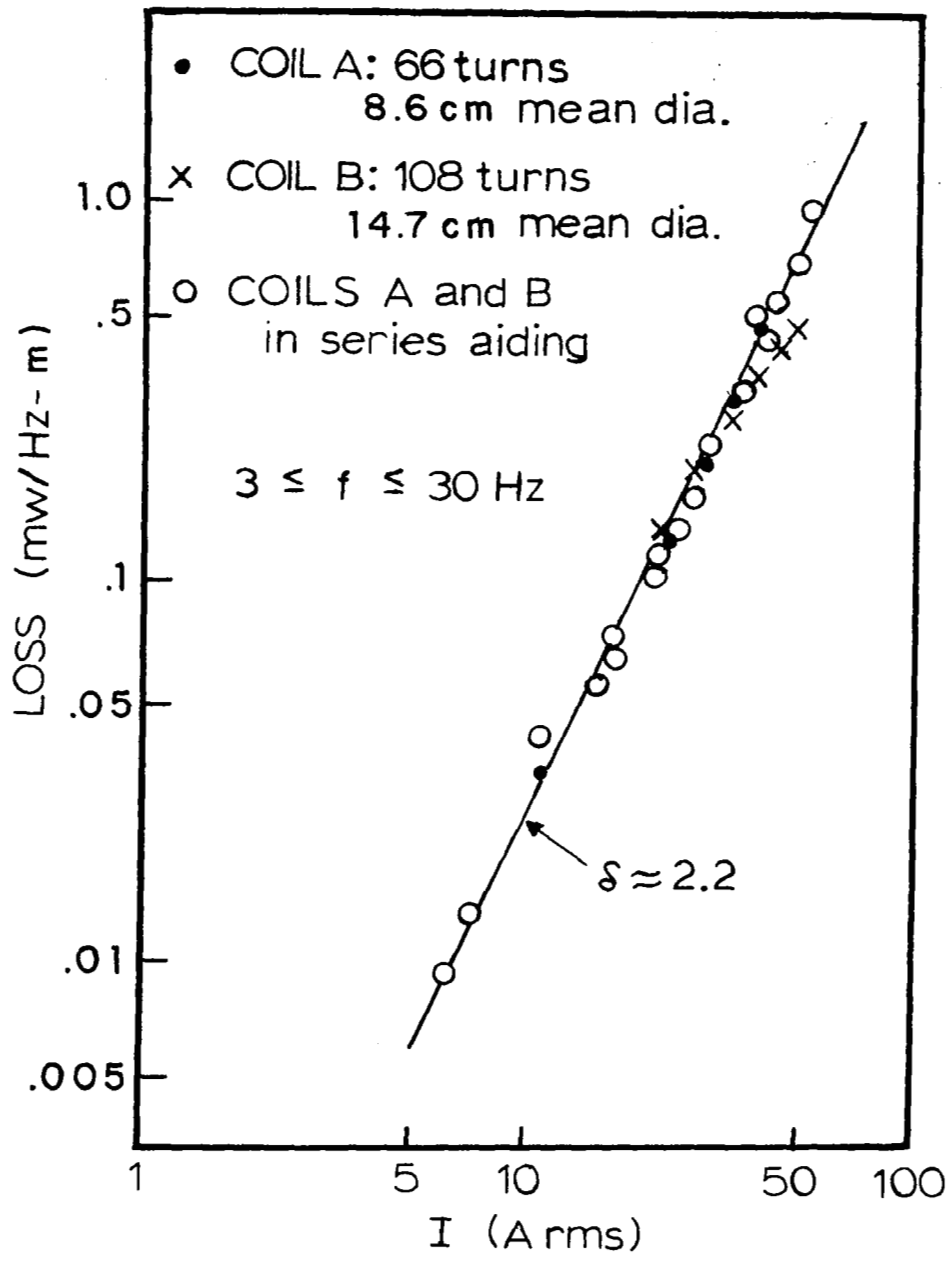

Figure 17 Results of A.C. Losses Scaling Tests.

aerodynamic tests were being considered and, hence, it would have been premature to decide on any particular coil configuration as being optimal in some sense. Rather, all calculations were made for a $\tan^{-1}\sqrt{8}$ configuration with drag augmentation similar to that of the improved prototype design. Also, a simple spherical model was used in the calculations as an adequate representative of the scale of more realistic aerodynamic shapes. Again, results presented below should be considered realistic from the point of view of order of magnitude only.

Before extrapolating design and operational characteristics of the prototype facility to large scale facilities, a redesign of the prototype coil assembly was carried out to take advantage of opportunities created by changes made during the development of the facility and lessons learned during the shake down and testing process. The principal changes that would be implemented in a new coil system are: (1) the main field coil would be split into a Helmholtz-like pair of coils with the same polarity to improve the uniformity of the magnetizing field in the vicinity of the nomimal suspension point, and (2) the drag augmentation coils would be moved closer to the suspension point and their windings would be located at a more favorable angle with respect to the coil axis, thus increasing the axial field gradient at NSP by nearly 50%. On the whole these changes result in a substantially more compact coil assembly than that of the existing prototype facility. This improved prototype design has been taken as the basis for the extrapolations discussed below. The principal coil dimensions for this optimized prototype configuration are given in Table 5.

TABLE 5

COIL	OD/ID/LENGTH (cm)	N Turns	# Coils
Main Field	48/40/4	1400	2
Drag Augmentation	50/38/6	3200	2
Gradient	20/12.7/1.3	135	6

4.3 Extrapolation to Larger Facilities

To understand the coil scaling process it is useful to remember that for a given geometric coil configuration, the magnitude of the magnetic force exerted by a pair of gradient coils on a magnetized sphere is of the form:

$$F_{MAG} = kVM \frac{\partial B_x}{\partial x}$$

where V, M, and $\frac{\partial B_x}{\partial x}$, have been defined before in this paper and k is a constant whose magnitude depends on the geometry of the gradient coil windings relative to the direction of magnetization and position of the sphere. Of course, in the case of air-core coils the magnitudes of magnetic fields and their gradients are simply proportional to the magnitudes of the respective currents. At the same time, aerodynamic forces are approximately proportional to the cross sectional area of a model. For example, for a sphere of diameter d the drag force exerted by a flow characterized by a dynamic pressure q is:

$$D = C_D \, q \frac{\pi d^2}{4}$$

From the scaling laws summarized in Figure 16 it follows that the magnitudes of magnetic field gradients remain constant for similar coil geometries while the magnitudes of magnetizing fields scale linearly with the coil characteristic dimension. Thus, assuming that the supported sphere's magnetization increases linearly with magnetizing field (a good approximation for iron in the range of magnetic field intensities of interest here), a practical expression for computing coil size requirements for larger but similarly shaped coil configurations is:

$$\frac{q1}{q2} \times \left(\frac{d2}{d1}\right) \times \lambda \left(\frac{NI2}{NI1}\right)_{MF} \times \frac{(NI2)_{DA} + \varepsilon (NI2)_{GRAD}}{(NI1)_{DA} + \varepsilon (NI1)_{GRAD}} = 1$$

where λ is the coil scaling factor (different, in general, from the model scaling factor) and ε represents the relative steady state contribution by the gradient coils to the magnetic force checking aerodynamic drag.

The contribution by the model weight has been neglected in this expression. Current density levels are assumed to remain unchanged and, hence, coil volumes scale with the magnitude of the product $\lambda(\frac{NI2}{NI1})$.

Coil size is important for three reasons. First, coil and cryostat costs should be dependent on size at least linearly. Second, steady state helium evaporation losses are expected to depend on wetted area and, hence, to scale roughly with the square of the coils (and therefore cryostat) characteristic dimension. Third, a.c. losses of gradient coils appear to scale linearly with the frequency of the changing current and the length of wound superconductor (see discussion in section 4.1).

Two specific examples of extrapolation to larger facilities have been chosen. Both are realistic in the sense that they involve either existing or planned aerodynamic test facilities (both at NASA Langley Research Center). Both are representative of the increased potential for utilization of magnetic suspension techniques brought about by the emerging cryogenic wind tunnel technology for high Reynolds number simulation.

Scaling to Langley Cryogenic Transonic Pilot Tunnel: This is a highly successful fully operational facility developed at NASA Langley Research Center to explore the design, operational, and research characteristics of the high Reynolds number cryogenic wind tunnel concept (10). From the point of view of investigating extensions of the magnetic suspension technique to large scale facilities, this facility offers the two main advantages of cryogenic wind tunnels, i.e., drastically reduced aerodynamic loads for a given Reynolds number (low q) and greatly reduced capital costs because of relatively small size. In this particular case, the intermediate size of the facility offers the additional advantage of providing the designer with an ideal size step in his design extrapolation.

A larger size, octagonal test section has been assumed available as a modification of the Transonic Pilot Tunnel, for the purposes of this exercise. Extreme (but realistic) flow conditions have also been

assumed. Results are presented in Table 6. A scaled sketch of the respective coil configurations is given as Figure 18 where the relative coil size reduction is evident, particularly for GRAD and DA coils. Thus, for example, although model volume increases by a factor of 64 and drag capability by a factor of 50, gradient coil volume and helium boil-off increase only by a factor of 8.

Note that in Figure 18 the linear scale of the sketch for the larger facility has been reduced by a factor of 4 to permit direct visual comparison with the optimized prototype facility. Hence, for example, it is apparent that substantial relative reductions in size of gradient coils and drag augmentation coils are possible even within the rather conservative assumptions stated above.

Scaling to Langley Cryogenic Transonic Research Tunnel: This is a truly large scale facility still in the design state at Langley Research Center. The only purpose of speculating this far into an as yet uncertain future is to explore to a practical upper limit the relative advantages of scaling a superconductor magnetic suspension while at the same time getting crude upper limit estimates of helium consumption. The last column in Table 6 summarizes the results of calculations based on straight extrapolation from the design for the Langley pilot facility. That is, no further relative reduction in cryostat or coil size is assumed. Estimated coil sizes and helium losses are expectedly quite large but do not appear forbidding in view of the size of the overall test facility. Furthermore, considerable improvements should be possible by a more elaborate design optimization process.

TABLE 6

Summary of Design Extrapolations to Large Scale Aerodynamic Facilities

PARAMETERS RELEVANT TO FACILITY SCALING	OPTIMIZED UVA PROTOTYPE	FOR LANGLEY TRANSONIC PILOT TUNNEL	FOR LANGLEY TRANSONIC RESEARCH TUNNEL
1. TUNNEL GEOMETRY			
Shape of test section	circular	octogonal	octogonal
size (m) x 10	diameter: 1.46	across flats: 6.10	across flats: 24.4
2. MODEL SCALING			
diameter: d	1	4	16
projected area: $\sim d^2$	1	16	256
volume: $\sim d^3$	1	64	4096
3. FLOW CHARACTERIZATION			
Mach number	3	1	1
stagnation pressure (atm)	3.4	5.0	4.0
dynamic pressure (kN/m^2)	59	188	154
4. SPHERE DRAG SCALING	1	50	660
5. COIL GEOMETRIES (MF/DA/GRAD)			
mean diameter (m) x 10	4.39/4.39/1.65	13.65/11.99/7.11	54.36/48.01/28.45
cross section (sq m) x 100	.160/.361/.048	1.61/.645/.089	6.45/2.06/2.84
volume (cu m) x 1000	2.21/4.98/.25	69.3/24.3/2.00	1110/311/25.6
mean half angle to axis (deg)	69/55/25	69/55/31	69/55/31
6. HELIUM ANNULUS GEOMETRY			
inner wetted diameter (m) x 10	2.4	8.0	32.0
outer wetted diameter (m) x 10	6.6	17.8	71.1
7. MAGNETIC FIELD SCALING			
required drag capability	1	50	660
model volume factor	1	64	4096
model magnetization factor	1	3.25	3.25
drag augmentation factor	1	.24	.05
gradient coil factor	1	.24	.05
8. HELIUM BOIL-OFF			
scaling factor for background losses	1	8.2	131
scaling factor for gradient coil losses	1	7.9	102
boil-off rate: (background/gradient coils/total) (ℓ/hr)	5/5/10	41/39/80	655/510/1165

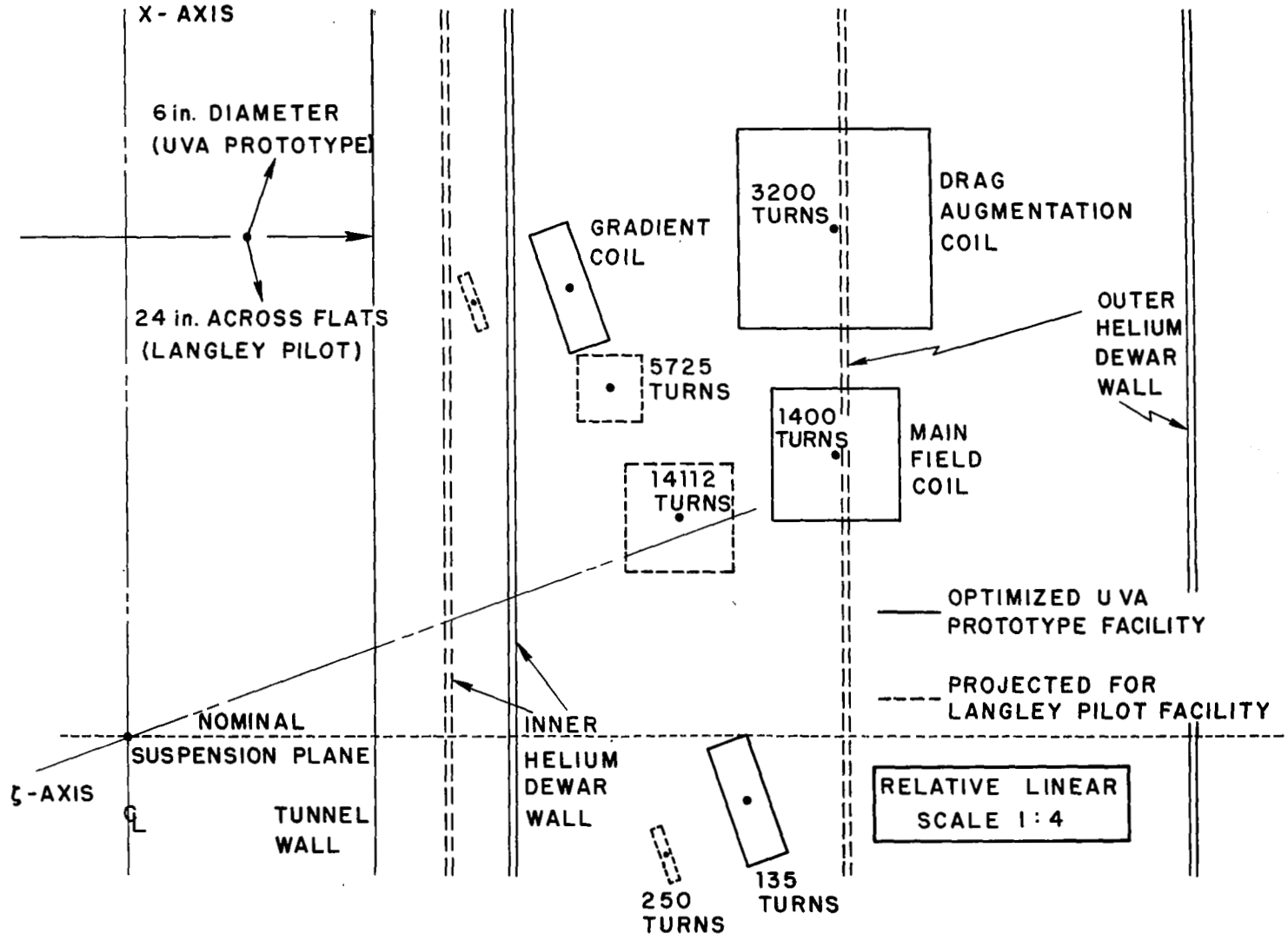

Figure 18 Design Extrapolation Dimensional Sketch.

4.4 Future Design Options

The superconductor magnetic suspension and balance prototype facility developed at the University of Virginia has served its main objective of proving the feasibility of this magnetic suspension concept. Technology relevant to implementing extrapolations of the technique to larger facilities has been explored. Much has been learned concerning design and operational characteristics of this type of facility. From this first-hand knowledge a list of problem areas where research efforts should be quite fruitful has emerged. A brief discussion on each item in this list follows:

Power Supplies: The one initial undesirable characteristic of the prototype power amplifiers is the noisy switching operation. Two immediate benefits will accrue from "smoother" power amplifiers, i.e., lower liquid helium evaporation rates and removal of the main obstacle in the way of a truly effective electromagnetic model position sensor. An additional feature to be explored concerns the feasibility of bi-directional power amplifier operation to reduce the average gradient coil operating current to zero.

Model Position Sensors: The shape-independent characteristic is very desirable. The potential of electromagnetic position sensors should be re-examined in the light of progress with noiseless power amplifiers.

Cryostat Design: As facilities become larger, background helium evaporation rates become significant. It is felt that much improvement can be made in this area. Also, the questions of tunnel accessibility and convertibility from a magnetic suspension mode to other tunnel operating modes must be examined in detail for large scale facilities.

Safety and Reliability: Again, the safety problem becomes more important as the scale of the facility grows larger. The area of reliability of magnetic suspension of wind tunnel models (as models become larger and more expensive) has not been studied in detail so far, but the economic incentive of doing so for larger systems is obvious.

Magnetic Coils: Better superconductors from the viewpoints of a.c. losses and current carrying capacity will obviously make the magnetic suspension technique more attractive for larger facilities. Given the overall low temperature environment furnished intermittently by cryogenic tunnels, the question of using non-superconductor coils should be re-examined as discussed in section 2.1.

Wind Tunnel/Magnetic Suspension Interface: Very significant improvements with respect to the prototype facility can be effected. Questions of accessibility for setting up and observation, convertibility to regular wind tunnel operation, and other relevant questions should be studied in considerable detail before freezing the design of larger facilities.

5. CONCLUSION

This project has been an unusually rewarding experience for this author and a host of co-workers who, at all levels of expertise and responsibility, have made the reported success of this proof-of-concept project possible. However, satisfaction of past accomplishments cannot compare with the sense of anticipation for what can be accomplished in the future. The technical breakthrough reported herein together with the spectacular success of the cryogenic wind tunnel concept have finally made the dream of a large-scale clean-tunnel aerodynamic testing truly feasible.

In view of the above, one cannot escape the conclusion that the logical next step should be to build a medium size facility where the design extrapolation estimates and the suggested improvements can be tested. All the necessary technology to carry out this next step is available today. Ideally, this intermediate scale facility would combine a superconductor magnetic suspension with a cryogenic wind tunnel, thus enabling sufficiently high Reynolds number experiments to be performed to assess quantitatively the merits of free-support aerodynamic testing in realistic flight simulation environments. The implementation of such proposal should prove a challenging and rewarding endeavor.

REFERENCES AND PUBLICATIONS

REFERENCES

1. Parker, H. M., Summary of ARL Symposium on Magnetic Wind Tunnel Model Suspension and Balance Systems, ARL Report 66-0135, edited by F. L. Daum, pp. 137-157, July 1966.

2. Zapata, R. N. and T. A. Dukes, pp. 1-25, Report on Ref. 1.

3. Parker, H. M., et al., "Theoretical and Experimental Investigation of a Three-Dimensional Magnetic Suspension Balance for Dynamic Stability Research in Wind Tunnels", Technical Report No. AST-4030-105-68U, Research Laboratories for the Engineering Sciences, University of Virginia, March 1968.

4. Zapata, R. N., Proceedings of the Second International Symposium on Electromagnetic Suspension, University of Southhampton report edited by M. Goodyer and M. Judd, 1972, Paper A.

5. Efferson, K. R., Review of Scientific Instruments, vol. 38, No. 12, pp. 1776-79, December 1967.

6. Stephens, T., paper G, Report of Ref. 4.

7. Fluid-Dynamic Drag, Sighard F. Hoerner, 1965. (published by author).

8. Covert, E. E., et al., "Magnetic Balance and Suspension Systems for Use with Wind Tunnels," chapter 2 of Progress in Aerospace Sciences, Volume 14, pp. 27-107, edited by D. Kuchemann, Pergamon Press, 1973. (This reference represents a brief but quite complete review of the basic principles, design concepts, and applications of magnetic suspension techniques for aerodynamic testing, and includes rather extensive reference lists.)

9. Moss, F. E., paper C1, Report of Ref. 4.

10. Kilgore, R. A., et al., "The Cryogenic Wind-Tunnel Concept for High Reynolds Number Testing", NASA Technical Note TN D-7762. December 1974.

PUBLICATIONS

a. Zapata, R. N., et al. "University of Virginia Superconducting Wind-Tunnel Balance", Journal of Applied Physics, vol. 42, No. 1, pp. 3-5, January 1971.

b. Group of papers contributed to the Second International Symposium on Electromagnetic Suspension, Southampton University, July 1971. These papers are included in the symposium proceedings, edited by M. Judd and M. Goodyer and published in 1972. Also published as main body for Final Technical Report for NASA Grant NGR-47-005-029, University of Virginia RLES Report No. ESS-4009-101-73U, edited by R. N. Zapata, February 1973.

Paper A: "The University of Virginia Superconducting Suspension and Balance Facility", by R. N. Zapata.

Paper C: "The Use of Superconductivity in Magnetic Balance Design", by F. E. Moss.

Paper K: "Data Acquisition and Reduction for the U. Va. Superconducting Magnetic Suspension and Balance Facility", by I. D. Jacobson, J. L. Junkins, and J. R. Jancaitis.

Paper Q4: "Electromagnetic Position Sensor for a Magnetically Supported Model in a Wind Tunnel" by W. R. Towler and F. E. Moss.

Paper Q9: "Safety Aspects of Superconducting Magnetic Suspension Systems", by R. N. Zapata.

Paper S: "The Use of Iron and Extended Applications of the U. Va. Cold Balance Wind Tunnel System", by H. M. Parker.

c. Zapata, R. N., et al., "Experimental Feasibility Study of the Application of Magnetic Suspension Techniques to Large-Scale Aerodynamic Test Facilities", AIAA paper no. 74-615, presented at the AIAA 8th Aerodynamic Testing Conference, Bethesda, Md. July 1974.

d. Humphris, R. R., et al., "Performance Characteristics of the U.Va. Superconducting Wind Tunnel Balance", paper presented at the Applied Superconductivity Conference, Chicago, Ill., October 1974.

APPENDIX

Illustrative Photographs of Prototype Facility

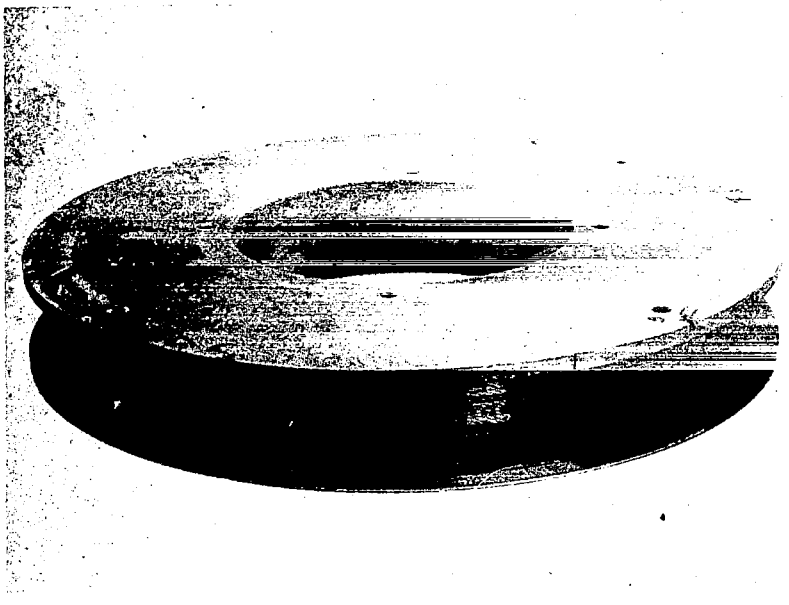

Drag Augmentation Coil

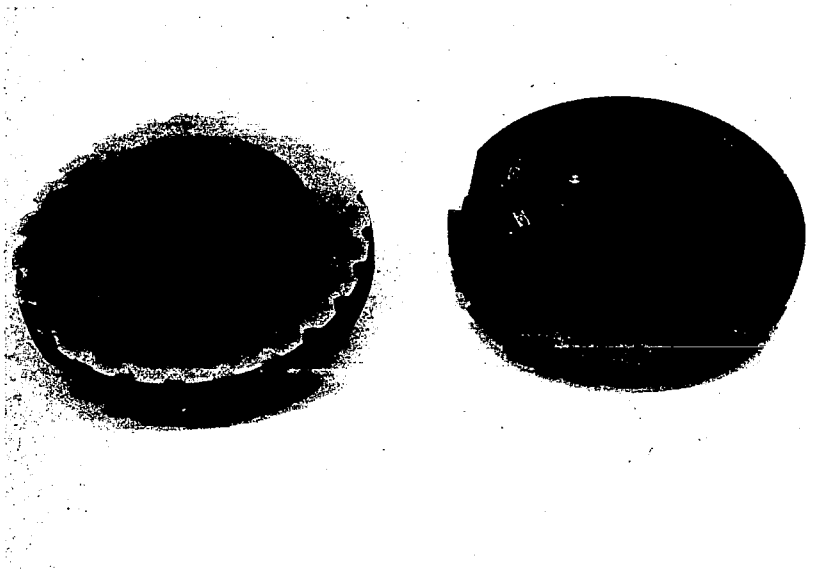

Gradient Coil

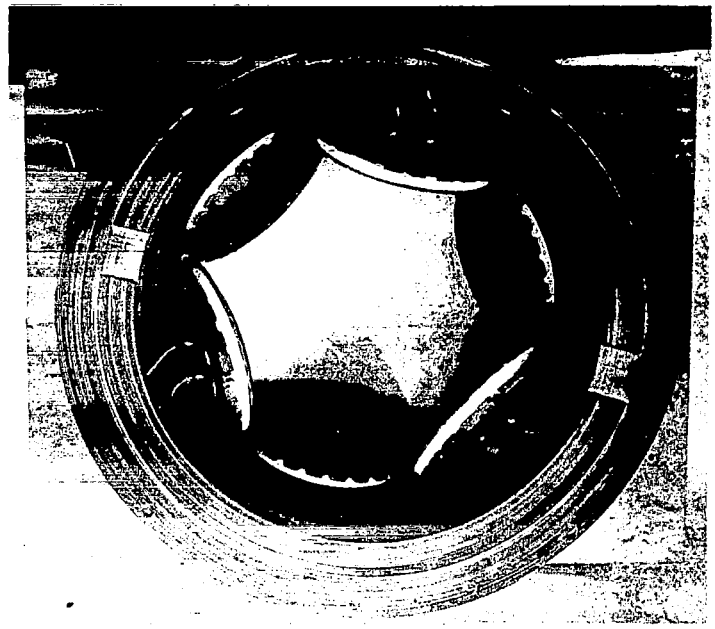

Gradient Coil Assembly (Top View)

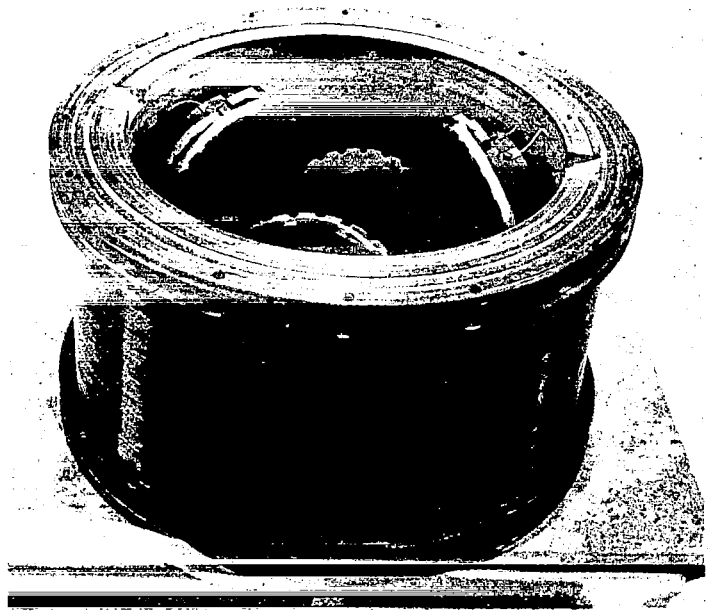

Main Field Coil

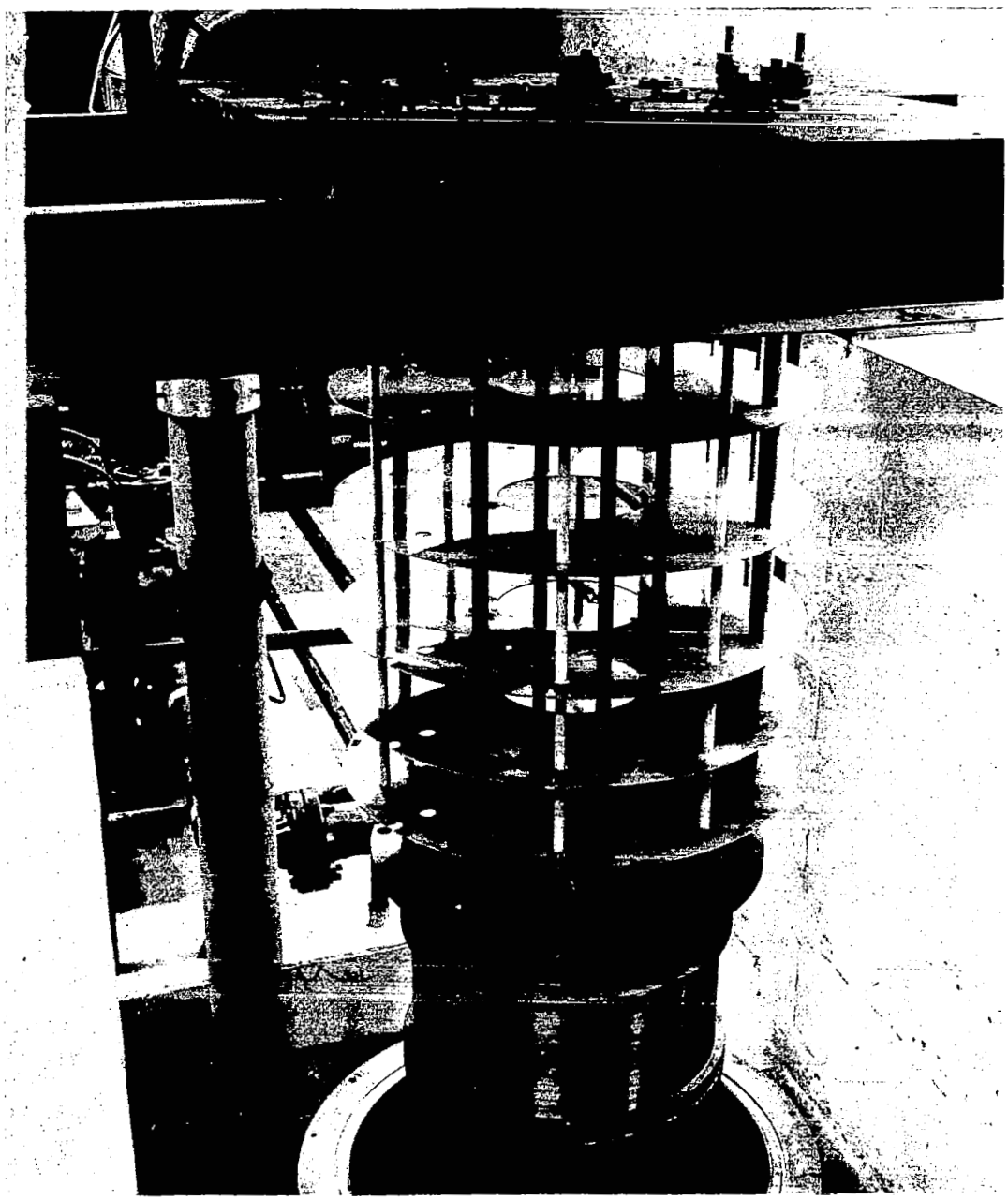

Coil Assembly and Radiation Shields Suspended from Top Plate

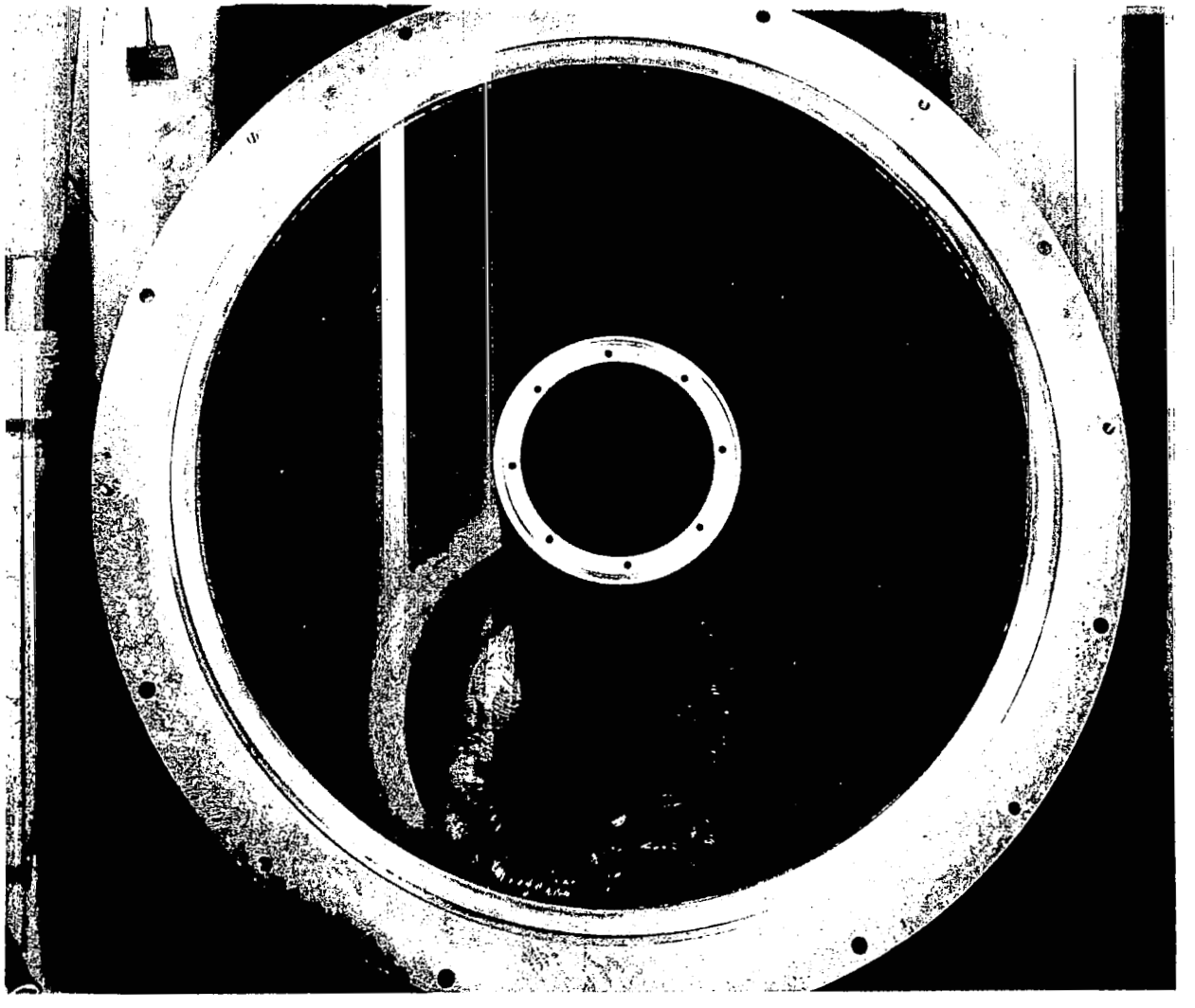

Inside of Helium Dewar

(Coil Assembly Fits in Bottom Annular Space)

General System View Including Power Amplifiers (extreme right) and Wind Tunnel Control Panel (foreground)